Center for Computational Engineering Science Mathematics Division

RWTH AACHEN UNIVERSITY

Diese Arbeit wurde vorgelegt am
Lehrstuhl für Mathematik (MathCCES)

Modellierung und numerische Simulation einer Kette neutraler Atome, welche mittels Anregung durch einen Laser kohärent an Rydberg Zustände gekoppelt werden

Modelling and numerical Simulation of a chain of neutral atoms coherently coupled to highly excited Rydberg states

Bachelorarbeit
Physik

Dezember 2020

Vorgelegt von Presented by	Nigel Nelles Rue du Bayehon 41, Ovifat, 4950 Weismes, Belgien Matrikelnummer: 298857 nigel.nelles@rwth-aachen.de
Erstprüfer First examiner	Prof. Dr. Benjamin Stamm Lehrstuhl für Mathematik (MathCCES) RWTH Aachen University
Zweitprüfer Second examiner	Prof. Dr. Stefan Weßel Lehr- und Forschungsgebiet Theoretische Physik (kondensierte Materie) RWTH Aachen University
Koreferent Co-supervisor	Loris Di Cairano Lehrstuhl für Mathematik (MathCCES) RWTH Aachen University

Eigenständigkeitserklärung

Hiermit versichere ich, dass ich diese Bachelorarbeit selbständig verfasst und keine anderen als die angegebenen Quellen und Hilfsmittel benutzt habe. Die Stellen meiner Arbeit, die dem Wortlaut oder dem Sinn nach anderen Werken entnommen sind, habe ich in jedem Fall unter Angabe der Quelle als Entlehnung kenntlich gemacht. Dasselbe gilt sinngemäß für Tabellen und Abbildungen. Diese Arbeit hat in dieser oder einer ähnlichen Form noch nicht im Rahmen einer anderen Prüfung vorgelegen.

Aachen, im Dezember 2020

Nigel Nelles

Contents

List of Figures

List of Tables

1. Abstract

In this thesis we have modeled a system consisting of an array of neutral atoms that are driven by lasers to highly excited Rydberg states. A numerical method to solve the model has been implemented and we were able to compute the ground state for systems of up to 20 atoms, which corresponds to a Hilbert space of more than a million dimensions. For systems of up to 15 atoms we successfully used the singular value decomposition to generate a reduced approximation space and to reduce the time needed to compute the ground state in a many-query context by more than a factor 500 while maintaining a precision of 99%. Using this decrease in computation time we plotted a diagram depicting information of 200 200 di erent ground states, corresponding to systems with di erent parameter values. For a system consisting of 15 atoms, the computation of this diagram took about 40 minutes on an average desktop computer. These diagrams depicting the ground state spectrum for di erent systems reveal that for certain sizes and parameter ranges, a speci c kind of translationally symmetric states makes up most of the ground state, with probabilities of 85%.

2. Introduction

Let us rst make an introduction on the topic, most information in this section comes from the two papers [2, 3]. The study of coherent many-body dynamics in arti cial systems is relatively new, since it is made possible by recent advances in technology allowing the control of the quantum state of individual quantum objects.
One of its uses would be to hopefully gain new insights in the eld of solid state physics. This could be done by quantum simulation, which means constructing systems that simulate the behavior of quantum objects in real matter. One advantage of these arti cial systems would be that it is possible to change the external parameters of the setup in ways that would not be possible with real matter. The parameters could for example be set to very high levels or be changed very suddenly. This could lead to the observation of new phenomenon that help us to better understand the behavior of matter on a quantum mechanical level.
These systems can also be used to simulate theoretical models, like the Ising model. Since the numerical simulation of quantum mechanical many-body systems is at the moment limited to about 50 particles, due to the exponential growth of the Hilbert space, simulation using interacting quantum objects can make it possible to examine larger systems than possible through numerical computation.
These arti cial systems also form the basis for the development of quantum computers. Basic elements of quantum processors have already been realized with di erent approaches, although only for a small number of coupled qubits. One example is trapped ions interacting through Coulomb interaction [25] where the qubits are encoded in atomic hyper ne levels. Two other examples are spins in semiconductors [1] and superconducting circuits [13]. Realizing quantum processors for a higher number of qubits proves to be a di cult challenge, the di erent requirements for this can be

found in [14].

One promising way to do quantum computing/quantum simulation is coherent coupling of neutral atoms to highly excited Rydberg states. The Rydberg state is a state where the outer electron is excited to a very high principal quantum number n. Since atoms in this state form a dipole they interact with each other through repulsive van-der-Waals interaction. As stated in [2] about the interaction between Rydberg atoms: "Such interactions have recently been used to realize quantum gates [33, 20, 29], to implement strong photon-photon interactions [28] and to study quantum many-body physics of Ising spin systems in optical lattices [30, 31, 34] and in probabilistically loaded dipole trap arrays [22]". The system that we are examining in this thesis is the same system constructed in [2], an array of several such atoms. The physical realization of this system can be done by locking atoms in a certain position with optical tweezers and exciting them with a laser.

Aside from the physical realization, it is also important to compute the theoretical behavior of such a system so that there is something to compare the real behavior to. The first part of the theoretical/numerical simulation would be to solve the stationary Schrödinger equation, which is what we will do in this thesis.
We will begin by introducing the mathematical framework needed to describe a quantum mechanical system, then we will look at the physics of an atom that is driven by a laser and see how that leads us to the Hamiltonian describing a multitude of such atoms interacting with each other. Before we proceed to the numerical analysis of the Hamiltonian we introduce the techniques used for the computation. Our simulation consists of computing the ground state spectrum of the Hamiltonian in a certain parameter range for different system sizes. Since every atom can be considered as a two-level quantum mechanical system, we find that the number of dimensions of the Hilbert space is 2^N, where N is the number of atoms in the array. We can see that the size of the Hilbert space is growing exponentially with the number of atoms and so is the time and memory needed for computations. Aside from the mathematical and physical perspective of the topic, the thesis will also deal with techniques to reduce the time and memory consumption of the computation within a many-query context. This will be just as important as the physical results, since the same techniques could be used to allow for more complex computations later on, like computing the temporal evolution of the system and maybe even use time-dependent parameters for the Hamiltonian.

3. Model

3.1. Dirac-Formalism

In this section we want to introduce the mathematical formalism that is used in quantum mechanics, the Dirac-Formalism. This section will focus solely on the mathematics, how it is used in physics will be covered in the section 3.2. The content of this section comes from different books [26, 18, 19, 32].

3.1.1. Hilbert Space

Let us begin by introducing the Hilbert space. It is the framework for the mathematics of quantum mechanics. We will start by introducing some definitions that are needed for the Hilbert space. The definition of the Vector space is [19]:

Definition 1 (Vector Space) A vector space over $\mathbb{C}$ consists of a set V along with two operations, the vector addition $+$ and the scalar multiplication $\cdot$. These two operations are subject to the conditions that for all vectors $\vec{u}, \vec{v}, \vec{w} \in V$ and all scalars $c, d \in \mathbb{C}$:

1. the set V is closed under vector addition, that is, $\vec{u} + \vec{v} \in V$
2. vector addition is commutative, $\vec{u} + \vec{v} = \vec{v} + \vec{u}$
3. vector addition is associative, $(\vec{u} + \vec{v}) + \vec{w} = \vec{u} + (\vec{v} + \vec{w})$
4. there is a zero vector $\vec{0} \in V$ such that $\vec{u} + \vec{0} = \vec{u}$ for all $\vec{u} \in V$
5. each $\vec{u} \in V$ has an additive inverse $\vec{w} \in V$ such that $\vec{u} + \vec{w} = \vec{0}$
6. the set V is closed under scalar multiplication, that is, $c \cdot \vec{u} \in V$
7. scalar multiplication distributes over scalar addition, $(c + d) \cdot \vec{u} = c \cdot \vec{u} + d \cdot \vec{u}$.
8. scalar multiplication distributes over vector addition, $c \cdot (\vec{u} + \vec{v}) = c \cdot \vec{u} + c \cdot \vec{v}$
9. ordinary multiplication of scalars associates with scalar multiplication, $(cd) \cdot \vec{u} = c \cdot (d \cdot \vec{u})$
10. multiplication by the scalar 1 is the identity operation, $1 \cdot \vec{u} = \vec{u}$

Note that for item (7), the $+$ on the left side means the addition of two complex numbers, while the $+$ on the right side means the addition introduced in the definition.

Definition 2 (Inner Product Space) An inner product space over $\mathbb{C}$ is a vector space over $\mathbb{C}$ with an inner product $\langle \cdot, \cdot \rangle$ that, for all vectors $\vec{u}, \vec{v} \in V$ and all scalars $c \in \mathbb{C}$, has the following properties [26]:

1. $\langle \vec{u}, \vec{v} \rangle = \langle \vec{v}, \vec{u} \rangle^*$ (* means the complex conjugate)

2. $\langle \tilde{\sigma}, \tilde{\tau}_1 + \tilde{\tau}_2 \rangle = \langle \tilde{\sigma}, \tilde{\tau}_1 \rangle + \langle \tilde{\sigma}, \tilde{\tau}_2 \rangle$

3. $\langle \tilde{\sigma}, c\,\tilde{\tau}_1 \rangle = c\langle \tilde{\sigma}, \tilde{\tau}_1 \rangle = \langle c^* \tilde{\sigma}, \tilde{\tau}_1 \rangle$

4. $\langle \tilde{\sigma}, \tilde{\sigma} \rangle \geq 0 \quad \forall\, \tilde{\sigma} \in V \quad (= 0 \text{ only for } \tilde{\sigma} = \tilde{0})$

At this point we want to introduce the Dirac notation. In this notation, vectors are written as $|\alpha\rangle, |\beta\rangle$ instead of $\tilde{\sigma}, \tilde{\tau}$. We can write the sum of two vectors $|\alpha\rangle, |\beta\rangle$ as $|\alpha\rangle + |\beta\rangle = |\alpha + \beta\rangle$ and the product of a scalar c and a vector $|\alpha\rangle$ as $c\,|\alpha\rangle = c|\alpha\rangle = |c\alpha\rangle$. For $|\alpha\rangle \in V$ we write the dual vector $\langle\alpha| \in V^*$ where V^* is the dual space. For a definition of the dual space, refer to [18]. For $|\alpha\rangle, |\beta\rangle \in V$, the inner product is written $\langle\alpha|\beta\rangle$.
In order to be able to define the Hilbert space, we need to introduce some more concepts [26].

Definition 3 (Norm) The norm of a vector $|\alpha\rangle$ is defined as

$$\|\alpha\| = \sqrt{\langle\alpha|\alpha\rangle} \in \mathbb{R}. \tag{1}$$

Definition 4 (Convergence) The sequence $\{|\alpha_n\rangle\}_{n\in\mathbb{N}} \subset V$ converges strongly towards $|\alpha\rangle \in V$ if

$$\lim_{n\to\infty} \|\alpha_n - \alpha\| = 0. \tag{2}$$

Definition 5 (Cauchy Sequence) A Cauchy sequence is defined as a sequence $\{|\alpha_n\rangle\}_{n\in\mathbb{N}} \subset V$ where there exists for each $\varepsilon > 0$, an $N(\varepsilon) \in \mathbb{N}$ so that

$$\|\alpha_n - \alpha_m\| < \varepsilon \quad \forall\, n, m > N(\varepsilon). \tag{3}$$

Definition 6 (Complete Vector Space) A vector space V is called complete, if every Cauchy sequence $\{|\alpha_n\rangle\}_{n\in\mathbb{N}} \subset V$ converges towards an element inside V.

Now we have everything we need to define the Hilbert space [18]

Definition 7 (Hilbert Space) A Hilbert space H is an inner product space over $\mathbb{C}$ which is also complete.

From now on we will be working in H instead of V. We will not specifically point out elements from H, H^*, or $\mathbb{C}$ most of the time. If not specified otherwise, every vector written in Dirac notation is meant to be an element of H or H^*, depending on the notation, and every lower case latin letter, with or without subscript, is an element of $\mathbb{C}$. Let us continue with some further definitions and theorems [26].

Definition 8 (Linear Independence) The vectors $|\alpha_1\rangle, |\alpha_2\rangle, \ldots, |\alpha_n\rangle$ are called linearly independent if the relation

$$\sum_{j=1}^{n} c_j |\alpha_j\rangle = |0\rangle \tag{4}$$

can only be fulfilled for $c_1 = c_2 = \ldots = c_n = 0$.

De nition 9 (Dimension of a Vector Space) The dimension of a Vector space H is de ned as the maximum number of linearly independent vectors in H.

De nition 10 (Orthogonality) $|i\rangle, |j\rangle$ are orthogonal if:

$$\langle j|i\rangle = 0. \tag{5}$$

De nition 11 A vector $|i\rangle$ is said to be normalized if $\langle k|k\rangle = 1$.

De nition 12 (Complete Orthonormal System) A complete orthonormal system (CONS) is de ned as a set $\{|\varphi_j\rangle\}$ of orthonormal vectors for which there does not exist an element in H, that does not belong to $\{|\varphi_j\rangle\}$, but is orthogonal to all elements of $\{|\varphi_j\rangle\}$.

We will sometimes call a CONS a complete set of orthonormal basis vectors or even just basis vectors. Orthonormal means orthogonal and normalized.

Theorem 1 If $\{|\varphi_j\rangle\} \subset H$ is a CONS, then we can write every vector $|i\rangle \in H$ as a linear combination of $\{|\varphi_j\rangle\}$:

$$|i\rangle = \sum_j c_j |\varphi_j\rangle. \tag{6}$$

For a proof of the nite-dimensional case, refer to [26], a proof of the in nite-dimensional case can be found in [32].

3.1.2. Linear Operators

In this section we want to de ne the di erent types of operators that we will be using later. The content of this section and the two sections that follow comes from [26], especially the de nitions. In order to distinguish operators from complex numbers, we will use capital letters for operators.

De nition 13 (Operator A) Mapping relation, which assigns to each element $|i\rangle$ from the partial set $D_A \subset H$ uniquely an element $|j\rangle \in W_A \subset H$:

$$|j\rangle = A|i\rangle = |Ai\rangle. \tag{7}$$

Sum and product of an operator are de ned as

$$(A_1 + A_2)|i\rangle = A_1|i\rangle + A_2|i\rangle; \quad |i\rangle \in D_{A_1} \cap D_{A_2}; \tag{8}$$

$$(A_1 A_2)|i\rangle = A_1(A_2|i\rangle); \quad |i\rangle \in D_{A_2};\ W_{A_2} \subset D_{A_1}. \tag{9}$$

De nition 14 (Operator $A^\dagger$ adjoint to A)

1. $D_{A^\dagger}$: Set of all $|i\rangle$ for which a $|\tilde{i}\rangle$ exists with:

$$\langle Aj|i\rangle = \langle \tilde{i}|j\rangle; \quad \forall |j\rangle \in D_A. \tag{10}$$

2. Mapping condition:

$$A^y|\ i\rangle = |\tilde{\ }i\rangle: \tag{11}$$

The adjoint operator has the following properties

1. There holds

$$\langle\ |A|\ i\rangle = \langle\ |A^y|\ i\rangle\ ;\quad |\ i\rangle 2\ D_A;\ |\ i\rangle 2\ D_{A^y}: \tag{12}$$

2. The adjoint operator A^y acts on $\langle\ |$ just like A acts on $|\ i\rangle$

$$\langle\ |A^y = \langle A\ |: \tag{13}$$

3. For suitable domains of de nition, which will not be indicated anymore from now on, we get

$$(A^y)^y = A: \tag{14}$$

4. The following identity holds,

$$(AB)^y = B^y A^y; \tag{15}$$

5. as well as

$$(A + B)^y = A^y + B^y; \tag{16}$$

$$(cA)^y = c\ A^y: \tag{17}$$

De nition 15 (Linear Operator A) An operator $A : D_A \to W_A$ is called linear if:

1. D_A is a linear subspace of H,
2. for arbitrary $|\ _1\rangle; |\ _2\rangle 2\ D_A$ it holds:

$$A(c_1|\ _1\rangle + c_2|\ _2\rangle) = c_1 A|\ _1\rangle + c_2 A|\ _2\rangle: \tag{18}$$

De nition 16 (Hermitian Operator A) An operator $A : D_A \to W_A$ is called hermitian if:

1. $D_A = D_{A^y} = H$,
2. $A = A^y \Leftrightarrow\ \ A|\ i\rangle = A^y|\ i\rangle\ \ 8|\ i\rangle 2 H$.

De nition 17 (Expectation Value) The expectation value of an operator A and a vector $|\ i\rangle$ is de ned as $\langle\ |A|\ i\rangle$.

3.1.3. Eigenvalue Problem

Now we want to treat the eigenvalue problem for operators and specifically look at the properties of the eigenspectrum of hermitian operators.

Definition 18 (Eigenvalue and Eigenvector) If $A|a_i\rangle = a|a_i\rangle$, then $|a_i\rangle$ is called an eigenvector of A with eigenvalue a.

Hermitian operators play a special role in quantum mechanics, this is because of four properties concerning their eigenvalues and eigenvectors.

Theorem 2 If A is a hermitian operator, then:

1. its expectation values are real.
2. its eigenvalues are real.
3. its eigenvectors are orthogonal.
4. its eigenvectors build a CONS.

Proof:

1. Let A be a hermitian operator and $|\psi\rangle$ an element of $\mathcal{H}$. Then
$$\langle\psi|A|\psi\rangle = \langle\psi|A^\dagger|\psi\rangle = \langle\psi|A|\psi\rangle^* \Rightarrow \langle\psi|A|\psi\rangle \in \mathbb{R} \quad \forall |\psi\rangle \in \mathcal{H}. \tag{19}$$
2. Let A be a hermitian operator and $|a_i\rangle$ an eigenvector of A with eigenvalue a. Then
$$\langle a_i|A|a_i\rangle = \langle a_i|a|a_i\rangle \Rightarrow a = \frac{\langle a_i|A|a_i\rangle}{\langle a_i|a_i\rangle}. \tag{20}$$
Since numerator and denominator are both real, a is also real.
3. For a proof, refer to [26].
4. For a proof, refer to [26] for the finite-dimensional case and [32] to find a deeper analysis for the infinite-dimensional case.

Theorem 3 It is possible to describe a hermitian operator A by its eigenvalues a_j and eigenvectors $|a_j\rangle$, this is called the spectral representation:
$$A = \sum_j a_j |a_j\rangle\langle a_j|. \tag{21}$$

Proof: Let A be a hermitian operator and $\{|a_j\rangle\}$ its eigenvectors which will always form a CONS. We can then write every vector $|\psi\rangle \in \mathcal{H}$ in this basis:
$$|\psi\rangle = \sum_j |a_j\rangle\langle a_j|\psi\rangle. \tag{22}$$

If we let the operator A act on $|\psi\rangle$ we get

$$A|\psi\rangle = \sum_j a_j |a_j\rangle\langle a_j|\psi\rangle. \tag{23}$$

Since this is true for every vector $|\psi\rangle \in \mathcal{H}$ we find

$$A = \sum_j a_j |a_j\rangle\langle a_j|. \tag{24}$$

Definition 19 (Identity Operator) The identity operator $\mathbb{1}$ is the operator that maps every state onto itself:

$$\mathbb{1}|\psi\rangle = |\psi\rangle \quad \forall |\psi\rangle \in \mathcal{H}. \tag{25}$$

It can be expressed in the spectral representation:

$$\mathbb{1} = \sum_j |a_j\rangle\langle a_j|. \tag{26}$$

We can insert the spectral representation of the identity operator in any expression without changing it.

3.1.4. Linear Operators as Matrices

Let $\{|u_j\rangle\}$ be a CONS, for an arbitrary vector $|\psi\rangle \in \mathcal{H}$ we can then assign a possibly infinite-dimensional column vector

$$|\psi\rangle \doteq \begin{pmatrix} a_1 \\ a_2 \\ \vdots \\ a_m \\ \vdots \end{pmatrix}, \tag{27}$$

where $a_j = \langle u_j|\psi\rangle$ are the projections of that vector onto the basis $\{|u_j\rangle\}$. To the dual vector $\langle\psi|$ we can now assign a possibly infinite-dimensional row vector

$$\langle\psi| \doteq \begin{pmatrix} a_1^* & a_2^* & \cdots & a_m^* & \cdots \end{pmatrix}. \tag{28}$$

We can define the inner product of two such vectors, where $|\varphi\rangle = \sum_j b_j |u_j\rangle$, as

$$\langle\psi|\varphi\rangle = \begin{pmatrix} a_1^* & a_2^* & \cdots & a_m^* & \cdots \end{pmatrix} \begin{pmatrix} b_1 \\ b_2 \\ \vdots \\ b_m \\ \vdots \end{pmatrix} = \sum_j a_j^* b_j. \tag{29}$$

and also de ne an outer product

$$|a\rangle\langle b| = \begin{pmatrix} a_1 \\ a_2 \\ \vdots \\ a_m \\ \vdots \end{pmatrix} \begin{pmatrix} b_1 & b_2 & \cdots & b_m \end{pmatrix} = \begin{pmatrix} a_1 b_1 & a_1 b_2 & \cdots & a_1 b_m & \\ a_2 b_1 & a_2 b_2 & \cdots & a_2 b_m & \\ \vdots & \vdots & \ddots & \vdots & \\ a_m b_1 & a_m b_2 & \cdots & a_m b_m & \\ \vdots & \vdots & & \vdots & \ddots \end{pmatrix}: \quad (30)$$

For an operator A we can write

$$A = 1A1 = \sum_{n;m} |u_n\rangle\langle u_n|A|u_m\rangle\langle u_m|; \quad (31)$$

which takes the form of a matrix

$$A = \begin{pmatrix} A_{11} & A_{12} & \cdots & A_{1m} & \\ A_{21} & A_{22} & \cdots & A_{2m} & \\ \vdots & \vdots & \ddots & \vdots & \\ A_{n1} & A_{n2} & \cdots & A_{nm} & \\ \vdots & \vdots & & \vdots & \ddots \end{pmatrix}; \quad (32)$$

where the matrix elements are de ned as $A_{nm} = \langle u_n|A|u_m\rangle$. We can get the elements of the adjoint operator A^y from $(A^y)_{nm} = A_{mn}$. For hermitian operators we nd the requirement $A_{nm} = A_{mn}$.

3.2. Physical Interpretation

Now that we have de ned the mathematical formalism, we want to specify how it is used in quantum mechanics. [26]

1. A quantum mechanical system is described by a Hilbert space.

2. A state in that system is described by a vector in that space.
   The number of dimensions that the Hilbert space has corresponds to the number of base states that the physical state can be made of.

3. An observable that can be measured is described by a hermitian operator.
   The reason we have to use operators to conduct a measurement is that in quantum mechanics, the in uence that the measurement has on the system can not be neglected. This is re ected in the fact that applying an operator to a vector, which describes the state, may alter it. We have to use hermitian operators, because its eigenvalues and expectation values, which also describe physical values, are real.

4. The possible results of the measurement are the eigenvalues of that operator.

5. When measuring the state of the system, the state gets filtered. If we have an operator $A = \sum_i a_i |a_i\rangle\langle a_i|$ and a state $|\psi\rangle = \sum_i b_i |a_i\rangle$, then after measuring a_i we have $|\psi\rangle = |a_i\rangle$.

6. The probabilities for measuring a_i are $|\langle a_i|\psi\rangle|^2$.
   For this reason, we will always consider normalized vectors.

There are some more concepts we want to introduce. The equation

$$\hat{H}|\psi\rangle = E|\psi\rangle; \tag{33}$$

where E is the energy of $|\psi\rangle$, is called the time-independent Schrödinger equation. It is also the eigenvalue equation of the operator $\hat{H}$, which is called Hamiltonian. The eigenvalues of $\hat{H}$ are the possible measurements for the energy of the system. There exists also a time-dependent Schrödinger equation, which is written

$$\hat{H}|\psi(t)\rangle = i\hbar|\dot{\psi}(t)\rangle: \tag{34}$$

The time-dependent Schrödinger equation describes the temporal evolution of a quantum mechanical state. If the Hamiltonian is not time-dependent, we can write the solutions of the time-dependent Schrödinger equation in terms of the solution to the time-independent one:

$$|\psi_i(t)\rangle = |\psi_i(t=0)\rangle e^{-iE_i t/\hbar}: \tag{35}$$

With $\hat{H}|\psi_i(t=0)\rangle = E_i|\psi_i(t=0)\rangle$ being a solution to the time-independent Schrödinger equation.

3.3. Many-Body Hilbert Space for Two-Level Particles

In this section we want to introduce the Hilbert space that describes a physical system composed of many two-level particles. Let us first begin with the Hilbert space of one such particle, it is a two-dimensional complex vector space.

3.3.1. Two-Level System

The two possible base states of our particle are the two orthonormal base vectors $|1\rangle = \begin{pmatrix}1\\0\end{pmatrix}$ and $|2\rangle = \begin{pmatrix}0\\1\end{pmatrix}$. Every possible state of that particle can be described as a combination of those two base states.

$$|\psi\rangle = c_1|1\rangle + c_2|2\rangle; \quad c_1, c_2 \in \mathbb{C}; \; \||\psi\rangle\|^2 = 1: \tag{36}$$

This system is equivalent to a two state spin system with $|\uparrow\rangle = \begin{pmatrix}1\\0\end{pmatrix}$ and $|\downarrow\rangle = \begin{pmatrix}0\\1\end{pmatrix}$.
Some important operators in a two-level system are the Pauli matrices. In a spin

system they can for example be used to measure the spin in any of the three spatial dimensions. The three Pauli matrices and the unit matrix are de ned as:

$$\mathbb{1} := |1\rangle\langle 1| + |2\rangle\langle 2| = \begin{pmatrix} 1 & 0 \\ 0 & 1 \end{pmatrix} \qquad \sigma_x := |1\rangle\langle 2| + |2\rangle\langle 1| = \begin{pmatrix} 0 & 1 \\ 1 & 0 \end{pmatrix}$$
$$\sigma_y := i(-|1\rangle\langle 2| + |2\rangle\langle 1|) = \begin{pmatrix} 0 & i \\ -i & 0 \end{pmatrix} \qquad \sigma_z := |1\rangle\langle 1| - |2\rangle\langle 2| = \begin{pmatrix} 1 & 0 \\ 0 & -1 \end{pmatrix}. \tag{37}$$

The pauli matrices have two eigenvalues each, +1 and −1, which are the possible measurements of the spin in the corresponding direction. The normalized eigenvectors corresponding to these eigenvalues are:

$$|+_x\rangle = \frac{1}{\sqrt{2}}\begin{pmatrix} 1 \\ 1 \end{pmatrix} = \frac{1}{\sqrt{2}}(|1\rangle + |2\rangle) \qquad |-_x\rangle = \frac{1}{\sqrt{2}}\begin{pmatrix} 1 \\ -1 \end{pmatrix} = \frac{1}{\sqrt{2}}(|1\rangle - |2\rangle)$$
$$|+_y\rangle = \frac{1}{\sqrt{2}}\begin{pmatrix} 1 \\ i \end{pmatrix} = \frac{1}{\sqrt{2}}(|1\rangle + i|2\rangle) \qquad |-_y\rangle = \frac{1}{\sqrt{2}}\begin{pmatrix} 1 \\ -i \end{pmatrix} = \frac{1}{\sqrt{2}}(|1\rangle - i|2\rangle) \tag{38}$$
$$|+_z\rangle = \begin{pmatrix} 1 \\ 0 \end{pmatrix} = |1\rangle \qquad |-_z\rangle = \begin{pmatrix} 0 \\ 1 \end{pmatrix} = |2\rangle.$$

3.3.2. Transition to the many Particle Hilbert Space

The notation $\mathcal{H}_1^{(i)}$ used in this section is taken from [27]. In [16] it is shown that Hilbert spaces can be combined using the tensor product and that is used as the Kronecker product when using the matrix formalism for operators. The de nition of the Kronecker product is:

De nition 20 (Kronecker Product) Let A be a $m \quad n$ matrix and B be a $p \quad q$ matrix. The matrix $C = A \quad B$ will then be an $mp \quad nq$ matrix with coe cients $C_{i'j'} = A_{ij} B_{kl}$ where $i' = (i \quad 1)\ p + k$ and $j' = (j \quad 1)\ q + l$.

Let us speci cally look at a composite Hilbert space that is the combination of N two-dimensional Hilbert spaces like the one we have just introduced. This composite Hilbert space will describe N particles that have two possible base states each. Let $\mathcal{H}_1^{(i)} \simeq \mathbb{C}^2$ be the Hilbert space of particle i and $\{|u_1^{(i)}\rangle, |u_2^{(i)}\rangle\}$ the orthonormal base of that Hilbert space $\mathcal{H}_1^{(1)}$. Then the Hilbert space of the N-particle system is de ned by $\mathcal{H}_N = \mathcal{H}_1^{(1)} \quad \mathcal{H}_1^{(2)} \quad \cdots \quad \mathcal{H}_1^{(N)} \simeq \mathbb{C}^{2^N}$. The complete set of orthonormal base vectors of the N-particle Hilbert space is composed of every possible combination of $\mathcal{H}_1^{(i)}$'s base vectors.

$$\left(\bigotimes_{i=1}^{N} |u_{\alpha_i}^{(i)}\rangle = |u_{\alpha_1}^{(1)}\rangle \quad |u_{\alpha_2}^{(2)}\rangle \quad \cdots \quad |u_{\alpha_N}^{(N)}\rangle = |u_{\alpha_1}^{(1)} u_{\alpha_2}^{(2)} \cdots u_{\alpha_N}^{(N)}\rangle \quad \alpha_i \in \{1, 2\}\right). \tag{39}$$

Every possible state $|\ \rangle \in \mathcal{H}_N$ can then be written as a linear product of these base vectors:

$$|\ \rangle = \sum_{\alpha_1, \alpha_2, \ldots, \alpha_N} C(\alpha_1, \ldots, \alpha_N) |u_{\alpha_1}^{(1)} u_{\alpha_2}^{(2)} \cdots u_{\alpha_N}^{(N)}\rangle. \tag{40}$$

The inner product of the N-particle Hilbert space is defined as,

$$\langle \psi | \phi \rangle = \left(\sum_{i_1, i_2, \ldots, i_N} C^*(i_1, \ldots, i_N) \langle u^{(1)}_{i_1} u^{(2)}_{i_2} \ldots u^{(N)}_{i_N} | \right) \left(\sum_{i_1, i_2, \ldots, i_N} C(i_1, \ldots, i_N) | u^{(1)}_{i_1} u^{(2)}_{i_3} \ldots u^{(N)}_{i_N} \rangle \right)$$
$$= \sum_{i_1, i_1', i_2, i_2', \ldots, i_N, i_N'} C^*(i_1, \ldots, i_N) C(i_1', \ldots, i_N') \, \delta_{i_1 i_1'} \delta_{i_2 i_2'} \ldots \delta_{i_N i_N'}. \tag{41}$$

where

$$| \psi \rangle = \sum_{i_1, i_2, \ldots, i_N} C(i_1, \ldots, i_N) | u^{(1)}_{i_1} u^{(2)}_{i_2} \ldots u^{(N)}_{i_N} \rangle. \tag{42}$$

If $A^{(i)}_1$ is an operator in $H^{(i)}_1$. Then the corresponding one-particle operator in H_N is defined as,

$$A^{(i)}_N = 1^{(1)}_1 \otimes \ldots \otimes 1^{(i-1)}_1 \otimes A^{(i)}_1 \otimes 1^{(i+1)}_1 \otimes \ldots \otimes 1^{(N)}_1 \tag{43}$$

3.4. Rabi Oscillations

In this section, by using the same derivation as presented in [11], we will examine the physics of a two-level quantum mechanical system interacting with an oscillatory perturbation. More specifically, we will study the case of an atom that is excited by a laser. We set the frequency of the laser close to the resonance frequency between the ground state $|1\rangle$ and a highly excited state $|2\rangle$. This way we can neglect the probabilities of the atom being in a different state than $|1\rangle$ or $|2\rangle$, making it an approximate two-level system. We can split the Hamiltonian of the system in an unperturbed part $\hat{H}^{(0)}$ which comes from the atom itself and a perturbation part $\hat{H}^{(1)}(t)$ which describes the excitation by a laser. The Hamiltonian $\hat{H}^{(0)}$ is defined as

$$\hat{H}^{(0)} = E_1 |1\rangle\langle 1| + E_2 |2\rangle\langle 2|. \tag{44}$$

$|1\rangle$ and $|2\rangle$ are the eigenstates of the Hamiltonian and E_1 and E_2 are the corresponding energies. We can write the temporal evolution of these states, which arises from the time-dependent Schrödinger equation:

$$|\psi^{(0)}_1\rangle = |1\rangle e^{-iE_1 t/\hbar}$$
$$|\psi^{(0)}_2\rangle = |2\rangle e^{-iE_2 t/\hbar}. \tag{45}$$

The perturbed Hamiltonian, containing the excitation by a laser is written as

$$\hat{H} = \hat{H}^{(0)} + \hat{H}^{(1)}(t). \tag{46}$$

Since the eigenfunctions (45) of the unperturbed Hamiltonian form a complete set, we can write any solution of the Schrödinger equation as a linear combination of those eigenfunctions:

$$|\psi^{(1)}\rangle = a_1(t)|1\rangle e^{-iE_1 t/\hbar} + a_2(t)|2\rangle e^{-iE_2 t/\hbar}. \tag{47}$$

Note that the coefficients are time-dependent, the composition of states changes over time. We will not further specify the time dependence of a_1 and a_2 from now on, as well as the time dependence of $|\Psi^{(1)}\rangle$. We can insert equation (47) into the time-dependent Schrödinger equation of the perturbed Hamiltonian (46) to get

$$\begin{aligned}
&(\hat{H}^{(0)} + \hat{H}^{(1)}(t))\,|\Psi^{(1)}\rangle = i\tilde{\hbar}\dot{\Psi}^{(1)}\rangle \\
\Leftrightarrow\quad & a_1\hat{H}^{(0)}|\psi_1^{(0)}\rangle + a_2\hat{H}^{(0)}|\psi_2^{(0)}\rangle + a_1\hat{H}^{(1)}|\psi_1^{(0)}\rangle + a_2\hat{H}^{(1)}|\psi_2^{(0)}\rangle \\
&= i\tilde{\hbar}(\dot{a}_1|\psi_1^{(0)}\rangle + \dot{a}_2|\psi_2^{(0)}\rangle + a_1\dot{\psi}_1^{(0)}\rangle + a_2\dot{\psi}_2^{(0)}\rangle) \\
\Leftrightarrow\quad & a_1\hat{H}^{(1)}|\psi_1^{(0)}\rangle + a_2\hat{H}^{(1)}|\psi_2^{(0)}\rangle = i\tilde{\hbar}(\dot{a}_1|\psi_1^{(0)}\rangle + \dot{a}_2|\psi_2^{(0)}\rangle);
\end{aligned} \tag{48}$$

where we have used the Schrödinger equation of the unperturbed Hamiltonian in the last step. We can further transform this equation by using (45), multiplying with $\langle\psi_1|$ and $\langle\psi_2|$ from the left and defining the resonance frequency $\omega_0 = \frac{E_2 - E_1}{\tilde{\hbar}}$,

$$\begin{aligned}
i\tilde{\hbar}\dot{a}_1 &= a_1\langle\psi_1|\hat{H}^{(1)}|\psi_1\rangle + a_2 e^{-i\omega_0 t}\langle\psi_1|\hat{H}^{(1)}|\psi_2\rangle \\
i\tilde{\hbar}\dot{a}_2 &= a_1 e^{i\omega_0 t}\langle\psi_2|\hat{H}^{(1)}|\psi_1\rangle + a_2\langle\psi_2|\hat{H}^{(1)}|\psi_2\rangle
\end{aligned} \tag{49}$$

Since the laser isn't changing the two energy levels E_1 and E_2 but only the occupation probabilities of the two states $|\psi_1\rangle$ and $|\psi_2\rangle$, the diagonal entries of $\hat{H}^{(1)}$ need to be 0 at anytime:

$$\langle n|\hat{H}|n\rangle = E_n = \langle n|\hat{H}^{(0)}|n\rangle + \langle n|\hat{H}^{(1)}|n\rangle = 0. \tag{50}$$

This simplifies the two equations (49) to

$$\begin{aligned}
i\tilde{\hbar}\dot{a}_1 &= a_2\langle\psi_1|\hat{H}^{(1)}|\psi_2\rangle e^{-i\omega_0 t}; \\
i\tilde{\hbar}\dot{a}_2 &= a_1\langle\psi_2|\hat{H}^{(1)}|\psi_1\rangle e^{i\omega_0 t}.
\end{aligned} \tag{51}$$

Let us now look more closely at $\hat{H}^{(1)}$. A laser can be described as an electromagnetic wave of the form

$$\vec{E}(\vec{r},t) = \vec{E}_0 e^{i(\vec{k}\cdot\vec{r} - \omega t)}. \tag{52}$$

Since the wavelength of the laser is much larger than the size of an atom, we can approximate the electromagnetic field to be constant over the space we are considering. We can simplify this expression further by only taking into account the real part, since the imaginary part does not influence our system.

$$\vec{E}(t) = \vec{E}_0\cos(-\omega t) = \vec{E}_0\cos(\omega t). \tag{53}$$

The outer electron forms a dipole with the core atom. The energy V of a dipole $\vec{p}$ in an electric field $\vec{E}(t)$ is

$$V(t) = -\vec{p}\cdot\vec{E}(t) = -q\vec{r}\cdot\vec{E}(t) \tag{54}$$

In our case, $\vec{r}$ becomes the operator $\hat{r}$ representing the direction and length of the dipole and the charge q is equal to e. This leads us to our Hamiltonian $\hat{H}^{(1)}(t)$:

$$\hat{H}^{(1)}(t) = -e\vec{E}(t) \cdot \hat{r} = -e\vec{E}_0 \cdot \hat{r}\cos(\omega t): \tag{55}$$

We are interested in the matrix elements of this Hamiltonian:

$$\langle 2|\hat{H}^{(1)}|1\rangle = -e\vec{E}_0\cos(\omega t)\langle 2|\hat{r}|1\rangle = \sim\cos(\omega t); \tag{56}$$

where we have defined

$$= \frac{e\vec{E}_0\langle 2|\hat{r}|1\rangle}{\sim} \tag{57}$$

as the Rabi frequency. As we will see later, the Rabi frequency is the frequency at which the probabilities of $|1\rangle$ and $|2\rangle$ oscillate back and forth, in the case of resonant driving. We can insert (56) into equation (51):

$$\begin{aligned} \dot{a}_1 &= -\frac{i}{2}a_2 e^{-i\omega_0 t}\cos(\omega t) = -\frac{i}{4}a_2(e^{-i(\omega_0+\omega)t} + e^{-i(\omega_0-\omega)t}); \\ \dot{a}_2 &= -\frac{i}{2}a_1 e^{i\omega_0 t}\cos(\omega t) = -\frac{i}{4}a_1(e^{i(\omega_0+\omega)t} + e^{i(\omega_0-\omega)t}): \end{aligned} \tag{58}$$

The frequency ω of our laser will be very close to the resonance frequency ω_0, this means that $\omega_0 - \omega \ll \omega_0 + \omega$. The two differential equations above show a superposition of two waves that differ in their frequency by several orders of magnitude. In the timescale of the oscillation $e^{i(\omega_0+\omega)t}$, the other oscillation $e^{i(\omega_0-\omega)t}$ will appear stationary because it is a lot slower. Whereas in the timescale of $e^{i(\omega_0-\omega)t}$, the faster oscillation will just even out because it is much faster. Since we are interested in the slower timescale, we will be neglecting the fast rotating terms, which is the so called rotating wave approximation (RWA). Without the fast rotating terms $e^{i(\omega_0+\omega)t}$, the equations become

$$\begin{aligned} \dot{a}_1 &\approx -\frac{i}{4}a_2 e^{i\Delta t}; \\ \dot{a}_2 &\approx -\frac{i}{4}a_1 e^{-i\Delta t}; \end{aligned} \tag{59}$$

where we have defined the detuning of the laser from the resonance frequency as

$$\Delta = \omega - \omega_0: \tag{60}$$

In order to solve this system of differential equations, we differentiate one and then substitute the other:

$$\ddot{a}_2 = -i\dot{a}_1\frac{}{4}e^{-i\Delta t} - a_1\frac{\Delta}{4}e^{-i\Delta t} = -\frac{\Delta}{4}\dot{a}_2 - i\frac{^2}{16}a_2: \tag{61}$$

We can solve this equation by using the ansatz $a_2 = e^{i\,t=2}(Ae^{iGt=2} + Be^{-iGt=2})$, which yields,

$$\begin{aligned} &\left(\frac{i}{2}G - \frac{i}{2}\right)^2 Ae^{i(G\ )t=2} + \left(\frac{i}{2}G - \frac{i}{2}\right)^2 Be^{i(-G\ )t=2} \\ &\qquad = \frac{j\ j^2}{4}(Ae^{i(G\ )t=2} + Be^{i(-G\ )t=2}) \\ &i\left(\frac{i}{2}G - \frac{i}{2}\right) Ae^{i(G\ )t=2} + \left(\frac{i}{2}G - \frac{i}{2}\right) Be^{i(-G\ )t=2}: \end{aligned} \tag{62}$$

We can split this equation into parts with A and parts with B, which gives the same results both times,

$$\begin{aligned} &\left(\frac{i}{2}G - \frac{i}{2}\right)^2 = \frac{j\ j^2}{4} - i\left(\frac{i}{2}G - \frac{i}{2}\right) \\ &) \quad \frac{1}{4}(G^2 + {}^2 - 2G) = \frac{1}{4}(j\ j^2 - 2G + 2{}^2) \\ &) \quad G^2 = j\ j^2 + {}^2: \end{aligned} \tag{63}$$

G is the generalized Rabi frequency. If we choose our initial condition to be $a_1(0) = 1$ and $a_2(0) = 0$, we get,

$$\begin{aligned} &a_2(0) = A + B = 0 \ ) \quad B = -A \\ &) \quad a_2 = 2iAe^{i\,t=2}\sin(Gt=2): \end{aligned} \tag{64}$$

We can insert this into the other di erential equation of (59),

$$\dot{a}_1 = -\frac{i}{2}a_2 e^{-i\ t} = -Ae^{-i\ t=2}\sin(Gt=2): \tag{65}$$

Integration of this expression gives us,

$$a_1(t) = \int_0^t -Ae^{-i\ t^0=2}\sin(Gt^0=2)dt^0 = \frac{2A}{-}e^{-i\ t=2}(G\cos(Gt=2) - i\sin(-Gt=2)): \tag{66}$$

We can use the normalization condition on these two functions,

$$\begin{aligned} |a_1|^2 + |a_2|^2 &= \left|\frac{2A}{-}e^{-i\ t=2}(G\cos(Gt=2) - i\sin(-Gt=2))\right|^2 + |2iAe^{-i\ t=2}\sin(Gt=2)|^2 \\ &= \frac{4A^2}{j\ j^2}(G^2\cos^2(Gt=2) + {}^2\sin^2(Gt=2)) + 4A^2\sin^2(Gt=2) = 4A^2\frac{G^2}{j\ j^2} \overset{!}{=} 1; \end{aligned} \tag{67}$$

which gives us $A = -=2G$ if we choose $$ to be real. Inserting this into our Ansatz we get the nal solution

$$a_1(t) = e^{-i\ t=2}(\cos(Gt=2) - \frac{i}{G}\sin(Gt=2)); \quad a_2(t) = e^{i\ t=2}\frac{i}{G}\sin(Gt=2): \tag{68}$$

If we analyze these expressions, we can see that the probabilities $|a_1|^2$ and $|a_2|^2$ are oscillating back and forth with the generalized Rabi frequency G. For the special case $= 0$, we have $G = $. In that case the system is driven by its resonant frequency, it completely oscillates back and forth between $|1\rangle$ and $|2\rangle$. The angular frequency of that oscillation between $|1\rangle$ and $|2\rangle$ is the Rabi frequency . If we have a detuning from the resonant frequency, $\neq 0$, the oscillation back and forth gets faster, but the amplitude of the oscillation decreases, which means that the probability $|a_2|^2$ never reaches one. This can be seen in gure 1.

Figure 1: Plot showing the Rabi oscillation for di erent . This plot was inspired by a plot in [11] depicting the same functions.

We also want to nd the Hamiltonian of the system. To do that, we start again at the set of di erential equations (51) and transform these by substituting $\tilde{a}_2 = e^{i t} a_2$:

$$\begin{aligned} i\dot{a}_1 &= \frac{1}{2} \quad \tilde{a}_2; \\ i\dot{\tilde{a}}_2 &= \frac{1}{2} \quad a_1 \quad \tilde{a}_2: \end{aligned} \tag{69}$$

If we write these equations in matrix form, we get a time dependent Schrödinger equation

$$i\frac{\partial}{\partial t}\begin{pmatrix} a_1 \\ a_2 \end{pmatrix} = \begin{pmatrix} 0 & \frac{\Omega}{2} \\ \frac{\Omega}{2} & \end{pmatrix}\begin{pmatrix} a_1 \\ a_2 \end{pmatrix} = \frac{1}{\tilde{}}\hat{H}\begin{pmatrix} a_1 \\ a_2 \end{pmatrix}; \tag{70}$$

with a Hamiltonian defined as

$$\frac{\hat{H}}{\tilde{}} = \begin{pmatrix} 0 & \frac{\Omega}{2} \\ \frac{\Omega}{2} & \end{pmatrix}: \tag{71}$$

This is our final result for the Hamiltonian of a two level system driven by a laser. The parameter Ω is a measure of the lasers intensity and ω is a measure of its frequency.

3.5. Array of strongly interacting neutral Atoms excited to Rydberg states

Some of the content/expressions in this section is deducted from previous sections, some is taken from [2, 3]. The system that we want to analyze in this thesis is a chain of equally spaced neutral atoms, that are coherently coupled to highly excited Rydberg states, with the help of lasers. It is the same system that is set up and examined in [2]. The laser is adjusted in a way that the atoms can only be in two states or a superposition of those, the ground state and the so called Rydberg state. The Rydberg state is a state in which the outer electron has a very high principal quantum number n. Each of these atoms can be seen as a two-level system but instead of $|1\rangle$ and $|2\rangle$ we will describe the states with $|g\rangle = |1\rangle$ and $|r\rangle = |2\rangle$. Rabi oscillations, which we have introduced in the previous section, describe the dynamics of the atoms driven by lasers. We have found that the one-particle Hamiltonian takes the form

$$\frac{H}{\tilde{}} = \frac{\Omega}{2}\sigma_x + \Delta\hat{n}: \tag{72}$$

where the operator $\hat{n}$ is defined as $\hat{n} = |r\rangle\langle r|$, and Δ is real. In order to find the Hamiltonian for N particles, we first have to transform the single-particle Hamiltonian of every atom to the N-particle Hilbert space $\mathcal{H}_N$. This transformation can be done according to (43). For atom i we get the Hamiltonian inside $\mathcal{H}_N$

$$\frac{H^{(i)}}{\tilde{}} = \frac{\Omega}{2}\sigma_x^i + \Delta\hat{n}_i; \tag{73}$$

where σ_x^i and $\hat{n}_i$ are the one-particle operators inside $\mathcal{H}_N$, which are transformed from σ_x and $\hat{n}$ according to (43). The Hamiltonian H for the whole system can be found by adding all of the single-atom Hamiltonians $H^{(i)} \in \mathcal{H}_N$ together:

$$\frac{H}{\tilde{}} = \frac{\Omega}{2}\sum_i \sigma_x^i + \sum_i \Delta\hat{n}_i: \tag{74}$$

In this thesis we are only considering the case where all of the atoms are driven with the same Rabi frequency and detuning, that is why we write and instead of $_i$ and $_i$. There is an additional term that we have to take into account, the interaction between atoms. At the distances we are examining, ground state atoms don't interact with each other, but Rydberg atoms form dipoles that interact through van-der-Waals interaction. Considering this interaction between Rydberg atoms, the Hamiltonian becomes

$$\frac{H}{\sim} = \frac{}{2} \sum_i \sum_x \hat{n}_i + \sum_{i<j} V_{ij} \hat{n}_i \hat{n}_j : \quad (75)$$

The interaction factor is de ned as $V_{ij} = C/R_{ij}^6$ [2, 3], where C is a constant and R_{ij} is the distance between the two atoms with index i and j. As we can see, the interaction factor decreases very rapidly as R_{ij} increases. This strong spatial variation of the interaction will prevent two atoms from being excited simultaneously if they are too close. The range at which two atoms can still be excited is speci ed by the Rydberg blockade radius R_b which is de ned as the range for which $V_{ij} = [2, 3]$, thus we nd $R_b = \sqrt[6]{C/}$. If two atoms are closer to one another than R_b, only one of the two will usually be excited, this e ect is called Rydberg blockade. Since our atoms are equally spaced, we can change the term R_{ij} to $V_{ij} = \frac{C}{((j\ i)a)^6}$, where a is the spacing between two neighbouring atoms. We can transform this further by introducing $n_S = \frac{R_b}{a}$, which gives us the Rydberg blockade range in number of atoms. $n_S = 2$ would for example mean that if an atom is excited to the Rydberg state, two neighbouring atoms on each side would have their excitation suppressed. With n_S we can transform V_{ij} to $V_{ij} = (\frac{n_S}{j\ i})^6$ which eliminates C. Our Hamiltonian then becomes

$$\frac{H}{\sim} = \frac{}{2} \sum_i \sum_x \hat{n}_i + \sum_{i<j} \left(\frac{n_S}{j\ i}\right)^6 \hat{n}_i \hat{n}_j : \quad (76)$$

Since the ground state spectrum is independent of a factor in front of H, we can simplify it further:

$$\frac{1}{\sim} H\ —; n_S = \frac{1}{2} \sum_i \sum_x — \sum_i \hat{n}_i + \sum_{i<j} \left(\frac{n_S}{j\ i}\right)^6 \hat{n}_i \hat{n}_j : \quad (77)$$

This is the nal form of the Hamiltonian. A physical construction of this system would have three external parameters, the intensity of the laser, which dictates , the frequency of the laser, which dictates and the spacing a between the atoms. In our model we chose to use and $n_S(\ ; a; C)$ as our two parameters, since only those in uence the ground state.

We are now nished constructing the model of the system we want to examine, the Hamiltonian (77) and the space H_N fully describe the system. In the next section, Computation, we are going to describe our approach to simulate the system. For us this will be equivalent to solving the eigenvalue problem of the constructed Hamiltonian

for different parameters. This would seem trivial at first glance, but since the dimensionality of $H \simeq \mathbb{C}^{2^N}$ grows exponentially with the number of atoms, it is important to use every possible way of speeding up the computation.

4. Computation

4.1. Constructing the Hamiltonian

The first step of the computation is to construct the Hilbert space and the Hamiltonian acting on it. Since the Hamiltonian we are interested in acts on a real-valued finite-dimensional space, we choose to work in the space $H \simeq \mathbb{R}^{2^N}$, where N is the number of atoms in our system. As stated in section 3.3.2, we can use the Kronecker product to construct the basis and operators of the many-particle Hilbert space based on the one-particle space and operators. If we choose the basis vectors of the one-particle systems to be

$$|g^{(i)}\rangle = \begin{pmatrix} 1 \\ 0 \end{pmatrix}; \quad |r^{(i)}\rangle = \begin{pmatrix} 0 \\ 1 \end{pmatrix}; \tag{78}$$

then we can construct the set of natural basis vectors

$$\{|u_i\rangle; 1 \le i \le 2^N\} \tag{79}$$

for the composite Hilbert space, where $|u_i\rangle$ denotes the vector with a 1 in ith coordinate and a 0 everywhere else. We find that the binary representation of the index $i-1$ corresponds to the state that base vector represents, if we replace 0 with g and 1 with r. If we take for example the case $N = 4$ and $i = 9$:

$$|u_9\rangle = |rggg\rangle \;\to\; \text{bin}(9-1) = \text{bin}(8) = 1000 \;\to\; rggg \tag{80}$$

This fact is quite convenient for the coding process, when having to make large vectors readable.

Now that we have covered the basis of the Hilbert space, let us look at how to construct the many-particle operators and with them the Hamiltonian. For $\hat{\sigma}_x^i$, according to (43), we find

$$\hat{\sigma}_x^i = \begin{cases} \sigma_x \otimes 1_{2^{N-1}}; & i = 1 \\ 1_{2^{i-1}} \otimes \sigma_x \otimes 1_{2^{N-i}}; & 1 < i < N \\ 1_{2^{N-1}} \otimes \sigma_x; & i = N \end{cases} \tag{81}$$

where $\sigma_x = \begin{pmatrix} 0 & 1 \\ 1 & 0 \end{pmatrix}$ and 1_k is the identity matrix in $\mathbb{R}^k$. For $\hat{n}_i$ we find equally

$$\hat{n}_i = \begin{cases} \hat{n} \otimes 1_{2^{N-1}}; & i = 1 \\ 1_{2^{i-1}} \otimes \hat{n} \otimes 1_{2^{N-i}}; & 1 < i < N \\ 1_{2^{N-1}} \otimes \hat{n}; & i = N \end{cases} \tag{82}$$

where $\hat{n} = \begin{pmatrix} 0 & 0 \\ 0 & 1 \end{pmatrix}$. With these building blocks we can construct the Hamiltonian (77).

The computation time just to construct this Hamiltonian increases quite drastically with the number of atoms. For the matrix multiplication $\hat{n}_i \hat{n}_j$ for example, there are $(2^N)^2 \cdot 2^N = (2^N)^3$ multiplications and $(2^N)^2 \cdot (2^N - 1) \approx (2^N)^3$ additions to be done. Together with the sum $\sum_{i<j} n_i n_j$ this becomes approximately $N! \cdot 2 \cdot (2^N)^3$ operations. For $N = 10$ that makes approximately $7.8 \cdot 10^{15}$ operations, for $N = 13$ it is already $6.8 \cdot 10^{21}$ operations. It is quite obvious that the computation will not get very far with such a high number of operations needed for $\sum_{i<j} \hat{n}_i \hat{n}_j$ alone.
Another problem is the amount of memory that is needed per matrix. For $N = 15$ we would need more than 8 GB for every single matrix, assuming that the matrices need 8 Byte per entry. The 30 single particle operators $\hat{x}_i$ and n_i would already need more than 240 GB together.

The size of the matrices, as well as the number of operations needed for Kronecker products and matrix multiplications can be drastically reduced however by using data structures and algorithms that make use of the fact that the matrices are quite sparse, which means that most of the matrices' elements are zero. An environment that is well suited for our needs is the programming language Python together with packages like NumPy [6, 5] and SciPy [9, 8]. SciPy offers, amongst a lot of other things, tools to construct and handle sparse matrices, this greatly reduces the time and memory needed to construct large Hamiltonians.

When we want to construct a lot of different Hamiltonians, we can reduce the time to do so further by constructing the Hamiltonian as a linear combination:

$$\frac{1}{\tilde{}}H(-, n_S) = \frac{1}{2}H_1 - H_2 + (n_S)^6 H_3, \tag{83}$$

where

$$H_1 = \sum_i \hat{x}_i, \quad H_2 = \sum_i \hat{n}_i, \quad H_3 = \sum_{i<j} \frac{1}{j - i}^6 \hat{n}_i \hat{n}_j. \tag{84}$$

If we want to construct the Hamiltonian for different parameter values, we only need to construct the three matrices H_1, H_2 and H_3 once and can then add them together for a lot of different parameter values $-$ and n_S. The sum (83) takes significantly less time to calculate than the whole calculation (77) and since H_1, H_2 and H_3 are stored as sparse matrices, they need very little memory.

That concludes the construction of the Hamiltonian, next we will describe how we compute its ground state.

4.2. Implicitly Restarted Lanzcos Method

In order to get the ground state of a constructed Hamiltonian, we are using a built-in function [10] of the SciPy package [8, 9]. As stated on the documentation page [10]: This function is a wrapper to the ARPACK [12] SSEUPD and DSEUPD functions which use the Implicitly Restarted Lanczos Method(IRLM) to nd the eigenvalues and eigenvectors. The Lanczos method is an iterative algorithm designed to nd a small number k of eigenvalues and corresponding eigenvectors of large symmetric matrices. A noteworthy feature of the Lanczos method is that the matrix coe cients do not need to be known, only its e ect when performing a matrix-vector multiplication. It would take quite long to properly introduce the method, which is why we are not treating it but use it as an established numerical method. Information on the original Lanczos method can be found in the paper by Cornelius Lanczos himself [23], for the modern implementation and the implicitly restarted variant refer to [24, 4].

4.3. Singular Value Decomposition

In this section we would like to describe the singular value decomposition(SVD) together with some of its properties [17], and how we can use it to speed up the computation of ground state vectors. First we would like to establish a speci c notation to describe a matrix A that is constructed of column vectors $\vec{a}_i$:

$$A = [\vec{a}_1 | \cdots | \vec{a}_n]: \tag{85}$$

Then we can de ne some elementary notions [17].

De nition 21 (Orthogonal Matrix) A matrix $A \in \mathbb{R}^{n\ n}$ is said to be orthogonal, if $AA^T = 1$. If $A = [\vec{a}_1 | \cdots | \vec{a}_n]$, then the vectors $\{\vec{a}_i\} \in \mathbb{R}^n$ form a CONS.

De nition 22 (span) Given a collection of vectors $\vec{a}_1, \ldots, \vec{a}_n \in \mathbb{R}$, the set of all linear combinations of these vectors is a subspace referred to as the span of $\vec{a}_1, \ldots, \vec{a}_n$:

$$\text{span}\{\vec{a}_1, \ldots, \vec{a}_n\} = \left(\sum_{j=1}^{n} {}_j \vec{a}_j \ : \ {}_j \in \mathbb{R} \right) \tag{86}$$

De nition 23 (Range) The range of a matrix $A = [\vec{a}_1 | \cdots | \vec{a}_n]$ is the subspace

$$\text{range}(A) = \text{span}\{\vec{a}_1, \ldots, \vec{a}_n\} \tag{87}$$

De nition 24 (Rank) The rank of a matrix A is de ned by

$$\text{rank}(A) = \dim(\text{range}(A)); \tag{88}$$

where $\dim(\text{range}(A))$ is the dimension of $\text{range}(A)$.

Theorem 4 If $A \in \mathbb{R}^{m \times n}$ is a real-valued matrix, then there exist orthogonal matrices

$$U \in \mathbb{R}^{m \times m}; \quad V \in \mathbb{R}^{n \times n} \tag{89}$$

such that

$$A = USV^T \tag{90}$$

where $S = \mathrm{diag}(s_1, s_2, \ldots, s_p) \in \mathbb{R}^{m \times n}$; $s_1 \geq s_2 \geq \ldots \geq s_p$ $p = \min(m, n)$.

This decomposition is called the SVD. The SVD is a generalization of the eigenvalue decomposition for non square matrices. Since U is orthogonal, its columns are basis vectors of $\mathbb{R}^m$. The entries s_i of the diagonal matrix S are called singular values.
As stated by Carl Eckart and Gale Young (Eckart-Young-Theorem) [15, 21], the SVD is the optimal way to approximate a matrix $A \in \mathbb{R}^{m \times n}$ of rank $p = \min(m, n)$, by a matrix $B \in \mathbb{R}^{m \times n}$ of rank $r < p$. The approximation can be done by first writing the SVD of A:

$$A = USV^T \tag{91}$$

where $S = \mathrm{diag}(s_1, s_2, \ldots, s_p) \in \mathbb{R}^{m \times n}$ and $U = [\vec{u}_1 | \ldots | \vec{u}_m]$. The approximated matrix B of rank r is then

$$B = US'V^T; \tag{92}$$

where $S' = \mathrm{diag}(s'_1, s'_2, \ldots, s'_p) \in \mathbb{R}^{m \times n}$ with

$$\begin{aligned} s'_i &= s_i \quad \forall i \leq r \\ s'_i &= 0 \quad \forall i > r \end{aligned} \tag{93}$$

A very useful property of a SVD of a matrix B with rank $r < p$ is that the set of vectors $\{\vec{u}_1, \ldots, \vec{u}_r\}$ is an orthonormal basis of the subspace $\mathrm{range}(B)$ [17].

Now that we have established these properties of the SVD and the SVD itself, we want to look at how we can use it to speedup the computation in a many-query context. We will be sticking to the normal vector notation in this section and write the ground state vector as $\vec{g}$ instead of $|g\rangle$.
Let us assume we have a Hamiltonian whose parameters $p_1, \ldots, p_l$ belong to a set W

$$H(p_1, \ldots, p_l) = H(\vec{p}) \in \mathbb{R}^{n \times n}; \qquad \vec{p} = \sum_{i=0}^{l} p_i \vec{e}_i; \ \vec{p} \in W \subset \mathbb{R}^l; \tag{94}$$

and that we wish to analyze the ground-state spectrum of this Hamiltonian as a function of the parameter $\vec{p}$. We could then compute the ground state $\vec{g}$ of $H(\vec{p})$ for a certain number k of values $\vec{p} \in W$. The points $\vec{p}$ should be equally distributed over W. If for a SVD of the matrix A that is constructed from these different ground states $\vec{g}$

$$A = USV^T; \quad A = [\vec{g}_1 | \ldots | \vec{g}_k] \tag{95}$$

we find that the singular values decay quickly enough:

$$s_r \ll s_1; \quad \text{for an } r < k \ll n; \tag{96}$$

then it is possible to approximate the matrix A with a matrix B of a lower rank, as stated by the Eckart-Young-Theorem. The set of vectors $\{\vec{u}_1, \ldots, \vec{u}_r\}$, which forms a basis of range(B) can then be used to approximately describe range$(A) = \text{span}(\vec{g}_1, \ldots, \vec{g}_k)$. This would mean that the k ground state vectors $\vec{g}_1, \ldots, \vec{g}_k$ can be described by a few basis vectors $\vec{u}_1, \ldots, \vec{u}_r$ where $r < k$. If this basis is suited to describe $\vec{g}_1, \ldots, \vec{g}_k$ it could hopefully be used to describe any ground state $\vec{g}$ of $H(\vec{p})$ where $\vec{p} \in W$. If we assume that this is the case, we can project the Hamiltonian $H(\vec{p})$ onto the space range$(B) = \text{span}(\vec{u}_1, \ldots, \vec{u}_r)$:

$$H_R(\vec{p}) = U_R^T H(\vec{p}) U_R \in \mathbb{R}^{r \times r}; \quad U_R = [\vec{u}_1 | \ldots | \vec{u}_r] \in \mathbb{R}^{n \times r}; \tag{97}$$

and compute the ground state of this reduced Hamiltonian $H_R(\vec{p})$ instead. If $\vec{g}_R \in \mathbb{R}^r$ is the ground state of $H_R(\vec{p})$, then we can find the approximated ground state $\vec{g}_A \in \mathbb{R}^n$ of $H(\vec{p})$ by projecting $\vec{g}_R$ to $\mathbb{R}^n$:

$$\vec{g}_A = U_R \vec{g}_R \tag{98}$$

Since $r \ll n$, this method would greatly reduce the dimension of the eigenvalue equation and with it the computation time.
We can not just assume that the basis vectors $\vec{u}_1, \ldots, \vec{u}_r$ are suited to describe any ground state for $\vec{p} \in W$ however. The validity of the approximation $\vec{g}_A \approx \vec{g}$ has to be verified. Before relying on the results $\vec{g}_A$ it is important to check $\|\vec{g}_A - \vec{g}\|$ for a meaningful number of ground states $\vec{g}$ that are different from the $\vec{g}$ that were used to find the basis $\{\vec{u}_1, \ldots, \vec{u}_r\}$.

For the actual computation of the SVD we use a built-in method [7] of the package NumPy.

5. Results

In the previous part, Computation, we have talked about the methods used to construct and analyze our Hamiltonian. In this part we are going to put those methods to use and analyze the results. First we will check for how big of a system we are able to construct the Hamiltonian and compute the ground state in an acceptable time. Then we will look at how well the SVD is suited to reduce the time of the ground state computation and how close these approximated ground states are to the exact ones. Finally we are going to compute the ground state spectrum of the Hamiltonian with the help of the SVD approximation by applying it in a many-query context.

5.1. Performance of Ground State Computation

In this section we want to look at how well our Code performs and at what system size it comes to its limits. For our computation we are using an Intel Core i5-7500 and 24 GB of DDR4 RAM clocked at 2400 MHz.

As described in the two sections 4.1 and 4.2, we construct the Hamiltonian

$$\frac{1}{\sim}H\ —; n_S = \frac{1}{2}\sum_i {}^{i}_{x}\ —\ \sum_i \hat{n}_i + \sum_{i<j} \frac{n_S}{j\ \ i}^{6} \hat{n}_i \hat{n}_j : \qquad (99)$$

and compute its ground state using the implicitly restarted Lanczos method. For the parameters we choose the following:

—	n_S
1	2.5

We measure the time it takes to construct this Hamiltonian and to compute the ground state, depending on the number of atoms. The results of the measurements are shown in gure 2. The construction time and the computation time are increasing exponen-

Figure 2: Plot showing the time needed to construct the Hamiltonian and to compute the ground state, depending on the system size. Time was measured for speci c parameter values.

tially with the number of atoms, as was to be expected, since the size of the Hilbert space$H \ ' \ R^{2^N}$ is increasing exponentially with the size as well.

The relationship between the ground state computation time and the two parameters – and n_S is not so straightforward. Depending on the value of those parameters, the ground state computation time varies over several orders magnitudes. The averaged computation time over di erent parameter values can be seen in gure 3. Note that since the standard deviation of the computation time is larger than the arithmetic mean, the error bar goes below zero. The time it takes to construct the Hamiltonian is independent of the parameters– and n_S.

Figure 3: Plot showing the time needed to compute the ground state, depending on the system size. Time was measured for several parameter values. The parameter values chosen are shown in gure 4 as $f s_{i;test} g$

5.2. Reducing computation time through SVD approximation

In this section we are going to look at how well the SVD is suited to approximate and speedup our computation. Our approach will be as described in section 4.3. We want to analyze the ground state spectrum for the following parameter and particle number range:

–	n_S	N_{Atoms}
0 5	0:5 4:5	11-15

Our parameter range forms a two-dimensional space W , with = on the x-axis and n_S on the y-axis. We choose equally spaced points $f s_{i;SV D} g$ in this parameter range

to build our matrix A. In order to test the accuracy of the SVD approximation afterwards, we use the points $\{\vec{n}_{i;test}\}$ which are located between the points $\{\vec{n}_{i;SVD}\}$. A representation of these points can be seen in figure 4.

First we compute the ground state $|g_i\rangle$ of every Hamiltonian $H(\vec{n})$, $\vec{n} \in \{\vec{n}_{i;SVD}\}$. Then we construct the matrix A which has all the ground states $|g_i\rangle$ as columns:

$$A = [g_1|\ldots|g_{45}]. \tag{100}$$

When A is constructed, we compute the SVD of $A = USV^T$, the singular values we have obtained this way are shown in figure 5. The decay of these singular values is good for every system size and almost does not grow while increasing the number of particles. This has an important consequence: the physics that is explored by the ground state under variation of the two parameters is not becoming more complex while increasing the number of particles. This is quite surprising as the dimension of the Hilbert space increases exponentially.
Now we want to test how well the first N_{Sing} columns of the matrix U work as basis to describe the ground states for our parameter range. To do this, we first compute the ground states $|g_i\rangle$ of every Hamiltonian $H(\vec{n})$ where $\vec{n} \in \{\vec{n}_{i;test}\}$. Then, for a specific N_{Sing}, we compute the approximated ground states $|\tilde{g}_i\rangle$ of the same Hamiltonians $H(\vec{n})$, $\vec{n} \in \{\vec{n}_{i;test}\}$, as described in the equations (97) and (98), where $r = N_{Sing}$.

We want to check how well the approximation performs in the worst case, which is why we are examining the maximum relative inaccuracy $_{max}(N_{Sing})$ over all our approximated ground states:

$$\begin{aligned} {}_{max}(N_{Sing}) &= \max(\{ {}_i\}); \\ {}_i &= \frac{\|\tilde{g}_i - g_i\|}{\|g_i\|}. \end{aligned} \tag{101}$$

Since $\|g\| = 1$ for any ground state, the division by $\|g\|$ is redundant, but it shows that the inaccuracy is relative. The results can be seen in figure 6, plots showing $_{mean}$ instead, with standard deviation, are in the Appendix section.

In figure 7, we have plotted the relationship $\overline{t_{gs;exact}}/\overline{t_{gs;approx}}$ for different values of N_{Sing}. $\overline{t_{gs;exact}}$ is the average computation time for an exact ground state and $\overline{t_{gs;approx}}$ is the average computation time for an approximated ground state. The times $t_{gs;exact}$ and $t_{gs;approx}$ were measured for all the different parameter values $\vec{n} \in \{\vec{n}_{i;test}\}$. The different measurements $t_{gs;exact}$ vary over several orders of magnitude which is why the standard deviation of $\overline{t_{gs;exact}}$ is bigger than $\overline{t_{gs;exact}}$ itself. This high deviation results in very large error bars for $\overline{t_{gs;exact}}/\overline{t_{gs;approx}}$, plots showing these can be found in the Appendix section.

Figure 4: Parameter values used for SVD approximation and for testing.

Figure 5: Singular Values of A.

Figure 6: Accuracy of the SVD approximation depending on the number N_{Sing} of singular values considered. $_{max}$ is the biggest relative inaccuracy across all the test points (see gure 4).

Figure 7: Plot showing the relationship $\overline{t_{gs;exact}} = \overline{t_{gs;approx}}$ for di erent numbers of atoms. $\overline{t_{gs;exact}}$ is the average time needed to compute an exact ground state. $\overline{t_{gs;approx}}$ is the average time needed to compute an approximated ground state, depending on N_{Sing}. N_{Sing} is the number of singular values considered for the SVD approximation.

The results of the SVD approximation are good, it can de nitely be used to speed up the computation while still beeing accurate enough. We choose $N_{Sing} = 20$, this

gives us an accuracy of about 99% while speeding up the computation by a factor 500 1000. In the following table we can see the times of the di erent parts of the computation for the chosen number of singular values $N_{Sing} = 20$:

N_{Atoms}	t_{Matrix}	t_{SVD}	$\overline{t_{constr}}$	$\overline{t_{gs;exact}}$	$\overline{t_{gs;approx}}$
11	34:7s	0:3s	(0:57 0:05)ms	(0:67 0:95)s	(0:90 0:02)ms
12	77:2s	1:2s	(0:82 0:11)ms	(1:47 2:02)s	(2:16 0:15)ms
13	161:8s	5:1s	(1:70 0:16)ms	(3:18 5:07)s	(3:78 0:25)ms
14	388:0s	20:8s	(3:20 0:10)ms	(6:94 12:10)s	(8:09 0:79)ms
15	1256:0s	87:7s	(7:36 2:53)ms	(21:53 31:74)s	(18:07 3:86)ms

t_{SVD} is the time needed to compute the SVD $A = USV^T$ and t_{Matrix} is the time it takes to compute the 45 ground states $jg_i i$ of $H(p); p 2 f p_{i;SVD} g$ and to construct the matrix

$$A = [g_1 j \cdots j g_{45}]: \tag{102}$$

$\overline{t_{constr}}$ is the average time it takes to construct the Hamiltonian, by using the linear combination (83). The time needed to compute H_1, H_2 and H_3 is very small compared to the total computation time, so it can be neglected. The di erent measurements of t_{constr} correspond to the parameter values $p 2 f p_{i;test} g$. $\overline{t_{gs;exact}}$ and $\overline{t_{gs;approx}}$ are as described before, in the table we can see quite well how large the standard deviation of computation time for exact ground states is.

It is important to mention that the ground state computation sometimes did not converge, this happened only for N_{Sing} 30. The corresponding times and accuracies were removed from the calculations. In the Appendix section are diagrams showing for each value of N_{Sing} how much of approximated ground state computations did not converge.

For a number n of ground state computations, we nd the time t_{Full} needed without SVD approximation and the time t_{approx} needed with SVD approximation:

$$\begin{aligned} t_{Full}(n) &= n \ (t_{constr} + t_{gs;exact}) \\ t_{approx}(n) &= t_{Matrix} + t_{SVD} + n \ (t_{constr} + t_{gs;approx}): \end{aligned} \tag{103}$$

The much faster computation time quickly makes up for the SVD's preparation time, the proportionality to n is about 300 times higher for t_{Full} than it is for t_{approx}.

5.3. Computation of the Spectrum

Now that we have found a way to quickly construct the Hamiltonian and compute its ground state, we can do so for a large number of parameter values and see what e ect

the parameters have on the ground state. Another challenge however, is depicting the relation between the parameters and the ground state. Since every ground state is a 2^N-dimensional vector

$$|g_i\rangle = \sum_{j=0}^{2^N} c_j |u_j\rangle; \tag{104}$$

there is no way to clearly represent such a vector as a whole. The most obvious way to examine a single ground state would be to sort the base states $|u_j\rangle$ by their probabilities $|c_j|^2$ and to look at the base states having the highest probability. In some cases, a single or a few base states make up the majority of the ground state $|g_i\rangle$. In other cases the ground state is a superposition of a lot of different possible base states with low probabilities each, then it is in a very uncertain state.

The way we have chosen to be the best to visually represent the relationship between the parameters and the ground state of the Hamiltonian is the following: We choose our two parameters $-$ and n_S as our two axes. For every point $(-; n_S)$ we represent a scalar $|c|^2_{max}(-; n_S)$ using colors. This scalar is calculated the following way: For our two parameters $(-; n_S)$ we construct the Hamiltonian and compute its ground state

$$|g_i\rangle = \sum_{j=0}^{2^N} c_j |u_j\rangle: \tag{105}$$

For this ground state we find the highest probability $|c_j|^2$ which will then be our scalar $|c|^2_{max}(-; n_S)$. These plots can be seen in figures 8 to 13. The problem with this representation is that it doesn't show which base state's probability is being depicted at what point, but the base state remains the same over larger areas and these areas are visually distinguishable from one another. We will add a small table to every plot that shows which areas correspond to which base states. In addition to this, there are larger tables in the Appendix section. These tables contain the probabilities of the 5 most probable base states for a number of points covering all of the different areas visible in the plots.

Before treating the plots of specific system sizes, let us make some general observations. There are two parts in the Hamiltonian that are competing, the sum $-\sum_i \hat{n}_i$ makes it favorable for the system to have as many excited atoms as possible in order to reduce the energy, but the sum $\sum_{i<j} (\frac{n_S}{j-i})^6 \hat{n}_i \hat{n}_j$ makes it favorable to reduce the number of closeby excitations. Depending on the number n_S, it will be favorable for two atoms with index i and j to be both excited if $|i - j| > n_S$, this effect scales with $-$. For low $-$, the ground state will be a superposition of a lot of low probability base states. With increasing $-$, the ground states will consist of fewer, higher probability base states, as certain patterns start to become a lot more favorable than others. Let us take a closer look at this case of higher $-$. For $n_S < 1$, the ground state

tends towards the single base state $|rrr:::rrr\rangle$, independent of the system size. For $1 < n_S < 2$ we find that for systems with an odd number of atoms, the ground state tends to go towards $|rgr:::rgr\rangle$, for an even number of atoms it becomes a superposition of states where half of the atoms are excited. In the case of $2 < n_S < 3$, we find that for system sizes $N = 3k + 1;\ k \in \mathbb{N}$, the ground state becomes for the most part $|rggrggrg:::grggr\rangle$. For other system sizes the ground state becomes a complex superposition of different base states.

We can generalize this concept, for $m - 1 < n_S < m$, a system with a number of atoms $N = mk + 1;\ k \in \mathbb{N}$ will form ground states that consist majorily of a base state having an excited atom at each end and forming a recurring pattern of one excited atom followed by $m - 1$ ground state atoms and starting again with an excited atom. Let us designate this pattern as Z_m symmetry. For system sizes that are not of the type $N = mk + 1;\ k \in \mathbb{N}$, in the range $m - 1 < n_S < m$, the ground state will form a superposition of several different base states. If a system size allows for Z_m symmetry, the ground state form $1 < n_S < m$ will always converge towards the corresponding base state.

Let us now look at specific system sizes. For every plot there will be a table showing which base states are being depicted in the different areas. In order to indicate the area, a single point in that area is specified, the base state corresponds to the whole area and not just the single point.

Figure 8: Diagram depicting $|c_j|^2_{max}$ for a system of size $N_{Atoms} = 11$

n_S	–	$\|u_j\rangle$
0:5	4:5	$\|rrrrrrrrrrr\rangle$ (Z_1)
1:5	4:5	$\|rgrgrgrgrgr\rangle$ (Z_2)
2:7	4:5	$\|rggrgggrggr\rangle$
4	4:5	$\|rggggrggggr\rangle$ (Z_5)

Starting with the case $N_{Atoms} = 11$ (gure 8). The base states corresponding to the di erent areas can be seen in the attached table. For this system size we can have ground states that form Z_1, Z_2 and Z_5 symmetry, as can be seen by the yellow areas in the plot. The phase of Z_5 symmetry goes even below $n_s = 4$. That is because the state $|rggggrggggr\rangle$ is the most energy e cient state, even when excited atoms with only three non-excited atoms between are allowed. The purple lines on the top and right border are due to non converging Lanczos computations.

Figure 9: Diagram depicting $|c_j|^2_{max}$ for a system of size $N_{Atoms} = 12$

n_S	–	$\|u_j\rangle$
0:5	4:5	$\|rrrrrrrrrrrr\rangle$ (Z_1)
1:6	4:5	$\|rgrgrggrgrgr\rangle$
2:3	4:5	$\|rggrggrgrggr\rangle$ and $\|rggrgrggrggr\rangle$
2:55	4:5	$\|rggrgggggrggr\rangle$
3:2	4:5	$\|rgggrggrgggr\rangle$
4:5	4:5	$\|rgggggrgggggr\rangle$ and $\|rggggrgggggr\rangle$

The plot for $N_{Atoms} = 12$ together with a table showing the corresponding base states can be seen in gure 9.

For this system size there can only be Z_1 symmetry, all other areas are relatively uncertain. In the table we can see quite well how the system tries to maximize the number of excited atoms and tries to minimize the interaction between excited atoms.

Figure 10: Diagram depicting $|c|^2_{max}$ for a system of size $N_{Atoms} = 13$

n_S	–	$\|u_j\rangle$
0:5	4:5	$\|rrrrrrrrrrrrr\rangle$ (Z_1)
1:6	4:5	$\|rgrgrgrgrgrgr\rangle$ (Z_2)
2:7	4:5	$\|rggrggrggrggr\rangle$ (Z_3)
3:7	4:5	$\|rgggrgggrgggr\rangle$ (Z_4)
4:7	4:5	$\|rgggggrgggggr\rangle$ (Z_6)

Figure 11: Diagram taken from [2], it depicts the ground state phase diagram for an array of 13 atoms. Comparison with gure 10 shows that we get similar results.

The diagram for $N_{Atoms} = 13$ is depicted in gure 10, as well as the corresponding table. For this system the ground state will be quite predictable for most parameters, since most of the time there is a con guration that is a lot more e cient than all others, which are the possible symmetries Z_1, Z_2, Z_3, Z_4 and Z_6. We can see that the area with Z_6 symmetry stretches down below $n_S = 5$, that is because this is also the most e cient way in the range $4 < n_S < 5$. When arranging excited atoms with at least four ground state atoms between, the best way to do so for maximizing the number of excited atoms and minimizing interaction between them is $|rggggrggggr\rangle$.
In the paper [2] they have shown a ground state phase diagram for the same system, it is shown in gure 11. Comparison with gure 10 shows that we get similar results.

Figure 12: Diagram depicting $|c_j|^2_{max}$ for a system of size $N_{Atoms} = 14$

n_S	–	$\|u_j\rangle$
0:7	4:5	$\|rrrrrrrrrrrrrr\rangle$ (Z_1)
1:6	4:5	$\|rgrgrgrggrgrgr\rangle$ and $\|rgrgrggrgrgrgr\rangle$
2:2	4:5	$\|rggrgrggrgrggr\rangle$
2:6	4:5	$\|rggrggrgggrggr\rangle$ and $\|rggrgggrggrggr\rangle$
3:7	4:5	$\|rgggrgggggrgggr\rangle$
4:7	4:5	$\|rgggggggrgggggr\rangle$ and $\|rgggggrggggggr\rangle$

The case $N_{Atoms} = 14$ (gure 12) is similar to $N_{Atoms} = 12$, we nd no possible sym-

metries except Z_1 and thus no base states that are dominant, except $|rrrrrrrrrrrrrrr\rangle$.

Figure 13: Diagram depicting $|c_j|^2_{max}$ for a system of size $N_{Atoms} = 15$

n_S	–	$\|u_j\rangle$
0.5	4.5	$\|rrrrrrrrrrrrrrr\rangle$ (Z_1)
1.6	4.5	$\|rgrgrgrgrgrgrgr\rangle$ (Z_2)
2.25	4.5	$\|rggrggrgrggrggr\rangle$
2.5	4.5	$\|rggrggrggggrggr\rangle$ and $\|rggrgggggrggrggr\rangle$
3	4.5	$\|rgggggrgggrgggggr\rangle$
4	4.5	$\|rgggggrgggrgggggr\rangle$

Finally $N_{Atoms} = 15$ (figure 13). For this system size only Z_1 and Z_2 symmetry is possible, thus we find no other base states being dominant.

Let us briefly mention the time needed to compute these diagrams. Each of these diagrams contains 200 200 pixels, for each pixel the Hamiltonian had to be constructed and the ground state computed as well as the highest probability found. In the following table we can see the computation times for different system sizes:

N_{Atoms}	t_{comp}
11	103.45s
12	181.92s
13	384.91s
14	854.26s
15	2236.8s

6. Conclusion

After setting up the basic mathematical formalism used in quantum mechanics we have modeled the system of an array of neutral atoms excited by lasers. Our Hamiltonian was parametrized by two parameters, the relation $\frac{\Delta}{\Omega}$ between the detuning and the Rabi frequency, as well as the number of suppressed Rydberg excitations m_s. The Hilbert space the Hamiltonian acts on grows exponentially with the number of atoms, which leads to the computation of the ground state becoming prohibitively expensive in a many-query context. In order to solve the computation time problem we projected the ground states onto a reduced space with lower dimension. We did this by applying a SVD to the space spanned by a set of different ground state vectors corresponding to Hamiltonians within a certain parameter range. This gave us a speedup of about two to three orders of magnitude which allowed us to reproduce observations of $\mathbb{Z}_2$-symmetry reported in [2]. The reduced space that we find does not grow significantly with the number of atoms when demanding the same accuracy and staying in the same parameter range. This suggests that the physics behind the ground states of the system does not get significantly more complex with the number of atoms, although the size of the Hilbert space grows exponentially.

7. Outlook

Since we reduced the computation time to a very low level, we would now have the freedom to add complexity to the computation. We could for example expand our computation to try to solve the time dependent Schrödinger equation. Another step could be to simulate the effect that a time-dependent Hamiltonian has on the system and simulate how the system behaves under quickly changing parameters.

A. Tables representing the ground state spectrum for di erent number of atoms

A.1. $N_{Atoms} = 11$

– = 0:5; n_S = 0:5	
$ju_j i$	$jc_j j^2$
jrrrrrrrrrrr i	0:027
jgrrrrrrrrrr i	0:018
jrrrrrrrrrrg i	0:018
jrgrrrrrrrrr i	0:011
jrrrrrrrrrgr i	0:011

– = 2:5; n_S = 0:5	
$ju_j i$	$jc_j j^2$
jrrrrrrrrrrr i	0:674
jrrrrrrrrgrr i	0:025
jrrgrrrrrrrr i	0:025
jrrrrrrgrrrr i	0:025
jrrrrgrrrrrr i	0:025

– = 4:5; n_S = 0:5	
$ju_j i$	$jc_j j^2$
jrrrrrrrrrrr i	0:869
jgrrrrrrrrrr i	0:012
jrrrrrrrrrrg i	0:012
jrgrrrrrrrrr i	0:011
jrrrrrrrrrgr i	0:011

– = 0:5; n_S = 1:5	
$ju_j i$	$jc_j j^2$
jrgggrgrgrgri	0:015
jrgrgrgrgggri	0:015
jrgggggggggir	0:015
jrgrgrgggrgri	0:015
jrgrgggrgrgri	0:015

– = 2:5; n_S = 1:5	
$ju_j i$	$jc_j j^2$
jrgrgrgrgrgr i	0:769
jrgrgggrgrgri	0:037
jrgrgrgggrgri	0:037
jrgggrgrgrgri	0:037
jrgrgrgrgggri	0:037

– = 4:5; n_S = 1:5	
$ju_j i$	$jc_j j^2$
jrgrgrgrgrgr i	0:901
jrgggrgrgrgri	0:018
jrgrgrgrgggri	0:018
jrgrgrgggrgri	0:018
jrgrgggrgrgri	0:018

– = 0:5; n_S = 2:7	
$ju_j i$	$jc_j j^2$
jgggggggggig	0:054
jrgggggggggi	0:050
jgggggggggir	0:050
jrgggggggggir	0:049
jgggggrgggir	0:023

– = 2:5; n_S = 2:7	
$ju_j i$	$jc_j j^2$
jrggrgggrggri	0:288
jrgggrggrggri	0:206
jrggrggrgggri	0:206
jrgggggrggir	0:053
jrggrgggggir	0:053

– = 4:5; n_S = 2:7	
$ju_j i$	$jc_j j^2$
jrggrgggrggri	0:431
jrgggrggrggri	0:235
jrggrggrgggri	0:235
jrgggggrggir	0:024
jrggrgggggir	0:024

– = 0:5; n_S = 4	
$ju_j i$	$jc_j j^2$
jgggggggggig	0:126
jgggggggggir	0:081
jrgggggggggi	0:081
jrgggggggggir	0:062
jgrgggggggig	0:040

– = 2:5; n_S = 4	
$ju_j i$	$jc_j j^2$
jrggggrggggir	0:661
jrgggggggggir	0:095
jrgggggrgggir	0:043
jrgggrgggggir	0:043
jrggggrgggig	0:036

– = 4:5; n_S = 4	
$ju_j i$	$jc_j j^2$
jrggggrggggir	0:902
jrgggggggggir	0:023
jrgggrgggggir	0:016
jrgggggrgggir	0:016
jrggggrgggig	0:015

A.2. $N_{Atoms} = 12$

– = 0:5; n_S = 0:5	
$\|u_j\rangle$	$\|c_j\|^2$
$\|rrrrrrrrrrrr\rangle$	0:020
$\|rrrrrrrrrrrg\rangle$	0:015
$\|grrrrrrrrrrr\rangle$	0:015
$\|rrrrrrrrrrgr\rangle$	0:008
$\|rgrrrrrrrrrr\rangle$	0:008

– = 2:5; n_S = 0:5	
$\|u_j\rangle$	$\|c_j\|^2$
$\|rrrrrrrrrrrr\rangle$	0:653
$\|rrgrrrrrrrrr\rangle$	0:024
$\|rrrrrrrrrgrr\rangle$	0:024
$\|rrrrgrrrrrrr\rangle$	0:024
$\|rrrrrrrgrrrr\rangle$	0:024

– = 4:5; n_S = 0:5	
$\|u_j\rangle$	$\|c_j\|^2$
$\|rrrrrrrrrrrr\rangle$	0:855
$\|rrrrrrrrrrrg\rangle$	0:012
$\|grrrrrrrrrrr\rangle$	0:012
$\|rrrrrrrrgrrr\rangle$	0:011
$\|rrrgrrrrrrrr\rangle$	0:011

– = 0:5; n_S = 1:6	
$\|u_j\rangle$	$\|c_j\|^2$
$\|rggggggggggr\rangle$	0:014
$\|rgggggggrgggr\rangle$	0:009
$\|rgggrgggggggr\rangle$	0:009
$\|rgggggggggrgr\rangle$	0:009
$\|rgrgggggggggr\rangle$	0:009

– = 2:5; n_S = 1:6	
$\|u_j\rangle$	$\|c_j\|^2$
$\|rgrgrggrgrgr\rangle$	0:210
$\|rgrggrgrgrgr\rangle$	0:169
$\|rgrgrgrggrgr\rangle$	0:169
$\|rggrgrgrgrgr\rangle$	0:076
$\|rgrgrgrgrggr\rangle$	0:076

– = 4:5; n_S = 1:6	
$\|u_j\rangle$	$\|c_j\|^2$
$\|rgrgrggrgrgr\rangle$	0:277
$\|rgrggrgrgrgr\rangle$	0:215
$\|rgrgrgrggrgr\rangle$	0:215
$\|rggrgrgrgrgr\rangle$	0:085
$\|rgrgrgrgrggr\rangle$	0:085

– = 0:5; n_S = 2:3	
$\|u_j\rangle$	$\|c_j\|^2$
$\|rggggggggggr\rangle$	0:036
$\|ggggggggggggg\rangle$	0:029
$\|ggggggggggggr\rangle$	0:028
$\|rgggggggggggg\rangle$	0:028
$\|rgggrgggggggr\rangle$	0:020

– = 2:5; n_S = 2:3	
$\|u_j\rangle$	$\|c_j\|^2$
$\|rggrgggggrggr\rangle$	0:159
$\|rggrggrgrggri\rangle$	0:103
$\|rggrgrggrggri\rangle$	0:103
$\|rggrggrggggr\rangle$	0:103
$\|rgggggrggrggr\rangle$	0:103

– = 4:5; n_S = 2:3	
$\|u_j\rangle$	$\|c_j\|^2$
$\|rggrggrgrggri\rangle$	0:242
$\|rggrgrgggrggri\rangle$	0:242
$\|rggrggrgggrgri\rangle$	0:118
$\|rgrggrggrggri\rangle$	0:118
$\|rggrgggggrggr\rangle$	0:061

– = 0:5; n_S = 2:55	
$\|u_j\rangle$	$\|c_j\|^2$
$\|rgggggggggggr\rangle$	0:042
$\|ggggggggggggg\rangle$	0:039
$\|rgggggggggggg\rangle$	0:035
$\|ggggggggggggr\rangle$	0:035
$\|rgggrgggggggg\rangle$	0:019

– = 2:5; n_S = 2:55	
$\|u_j\rangle$	$\|c_j\|^2$
$\|rggggrgggrggr\rangle$	0:134
$\|rggrggggrgggr\rangle$	0:134
$\|rggrgggggrggr\rangle$	0:124
$\|rggggrggrgggr\rangle$	0:107
$\|rggrggrgggggr\rangle$	0:071

– = 4:5; n_S = 2:55	
$\|u_j\rangle$	$\|c_j\|^2$
$\|rggrgggggrggr\rangle$	0:228
$\|rggrggggrgggr\rangle$	0:131
$\|rgggggrggrggr\rangle$	0:131
$\|rggggrggrggri\rangle$	0:119
$\|rggrgrggrggri\rangle$	0:119

– = 0:5; n_S = 3:2	
$\|u_j\rangle$	$\|c_j\|^2$
$\|ggggggggggggg\rangle$	0:074
$\|rgggggggggggg\rangle$	0:054
$\|ggggggggggggr\rangle$	0:054
$\|rgggggggggggr\rangle$	0:053
$\|gggggggggggrg\rangle$	0:024

– = 2:5; n_S = 3:2	
$\|u_j\rangle$	$\|c_j\|^2$
$\|rggggrggrgggr\rangle$	0:241
$\|rggrggggrgggr\rangle$	0:133
$\|rggggrgggrggr\rangle$	0:133
$\|rgggggggrgggr\rangle$	0:128
$\|rggggrggggggr\rangle$	0:128

– = 4:5; n_S = 3:2	
$\|u_j\rangle$	$\|c_j\|^2$
$\|rggggrggrgggr\rangle$	0:394
$\|rggrggggrgggr\rangle$	0:231
$\|rggggrgggrggr\rangle$	0:231
$\|rgggggggrgggr\rangle$	0:040
$\|rggggrggggggr\rangle$	0:040

– = 0:5; n_S = 4:5	
$\|u_j\rangle$	$\|c_j\|^2$
jggggggggggiggi	0:139
jrgggggggggigi	0:077
jgggggggggigiri	0:077
jrgggggggggiri	0:064
jgrgggggggigi	0:038

– = 2:5; n_S = 4:5	
$\|u_j\rangle$	$\|c_j\|^2$
jrgggggrgggiri	0:340
jrggggrgggigiri	0:340
jrgggggggggiri	0:100
jrgggggrgggigi	0:021
jgggggrgggigiri	0:021

– = 4:5; n_S = 4:5	
$\|u_j\rangle$	$\|c_j\|^2$
jrgggggrgggiri	0:442
jrggggrgggigiri	0:442
jrgggggggggiri	0:044
jrgggggrgggigi	0:009
jgggggrgggigiri	0:009

A.3. N_{Atoms} = 13

– = 0:5; n_S = 0:5	
$\|u_j\rangle$	$\|c_j\|^2$
jrrrrrrrrrrrri	0:014
jrgrrrrrrrrri	0:008
jrrrrrrrrrrgri	0:008
jrrrgrrrrrrri	0:007
jrrrrrrrrgrri	0:007

– = 2:5; n_S = 0:5	
$\|u_j\rangle$	$\|c_j\|^2$
jrrrrrrrrrrri	0:633
jrrgrrrrrrrri	0:023
jrrrrrrrrrgri	0:023
jrrrrgrrrrrri	0:023
jrrrrrrrrgrri	0:023

– = 4:5; n_S = 0:5	
$\|u_j\rangle$	$\|c_j\|^2$
jrrrrrrrrrrri	0:838
jrrrrrrrrrgri	0:012
jrrrgrrrrrrri	0:012
jrrrrrgrrrrri	0:012
jrrrrrrrgrrri	0:012

– = 0:5; n_S = 1:6	
$\|u_j\rangle$	$\|c_j\|^2$
jrgggggggggiri	0:011
jrgggggrgggiri	0:007
jrgggggggggigi	0:007
jgggggggggiri	0:007
jrgggggggrgiri	0:007

– = 2:5; n_S = 1:6	
$\|u_j\rangle$	$\|c_j\|^2$
jrgrgrgrgrgri	0:719
jrgrgrgggrgri	0:036
jrgrgrgrgggri	0:036
jrgrgggrgrgri	0:036
jrgrgrgrgggri	0:036

– = 4:5; n_S = 1:6	
$\|u_j\rangle$	$\|c_j\|^2$
jrgrgrgrgrgri	0:873
jrgrgggrgrgri	0:019
jrgrgrgrgggri	0:019
jrgrgrgggrgri	0:019
jrgrgrgrgggri	0:019

– = 0:5; n_S = 2:7	
$\|u_j\rangle$	$\|c_j\|^2$
jgggggggggggigi	0:036
jrgggggggggiri	0:035
jrgggggggggigi	0:033
jgggggggggiri	0:033
jrgggggggrgiri	0:016

– = 2:5; n_S = 2:7	
$\|u_j\rangle$	$\|c_j\|^2$
jrggrggrggrgri	0:722
jrggrgggggrgiri	0:047
jrgggggrggrgiri	0:046
jrggrggrgggiri	0:046
jgggrggrggrgiri	0:027

– = 4:5; n_S = 2:7	
$\|u_j\rangle$	$\|c_j\|^2$
jrggrggrggrgri	0:877
jrggrggrgggiri	0:026
jrgggggrggrgiri	0:026
jrggrgggggrgiri	0:026
jgggrggrggrgiri	0:018

– = 0:5; n_S = 3:7	
$\|u_j\rangle$	$\|c_j\|^2$
jgggggggggggigi	0:081
jrgggggggggiri	0:060
jgggggggggigiri	0:060
jrgggggggggigi	0:060
jgrgggggggggigi	0:026

– = 2:5; n_S = 3:7	
$\|u_j\rangle$	$\|c_j\|^2$
jrgggrgggrgiri	0:598
jrgggrgggggiri	0:095
jrgggggggrgiri	0:095
jggggrgggrgiri	0:035
jrgggrgggrgigi	0:035

– = 4:5; n_S = 3:7	
$\|u_j\rangle$	$\|c_j\|^2$
jrgggrgggrgiri	0:902
jrgggggggrgiri	0:027
jrgggrgggggiri	0:027
jggggrgggrgiri	0:016
jrgggrgggrgigi	0:016

– = 0:5; n_S = 4:7	
$\|u_j\rangle$	$\|c_j\|^2$
|ggggggggggggg⟩	0:135
|ggggggggggggr⟩	0:067
|gggggggggggrg⟩	0:067
|ggggggggggrgg⟩	0:045
|gggggggggggrr⟩	0:036

– = 2:5; n_S = 4:7	
$\|u_j\rangle$	$\|c_j\|^2$
|gggggrgggggrr⟩	0:467
|gggggggrgggggr⟩	0:090
|gggggrgggggrg⟩	0:090
|gggggggggggrg⟩	0:087
|gggggrgggggrg⟩	0:028

– = 4:5; n_S = 4:7	
$\|u_j\rangle$	$\|c_j\|^2$
|gggggrgggggrr⟩	0:791
|gggggrgggggrg⟩	0:049
|gggggggrgggggr⟩	0:049
|gggggggggggrg⟩	0:038
|gggggrgggggrg⟩	0:017

A.4. N_{Atoms} = 14

– = 0:5; n_S = 0:5	
$\|u_j\rangle$	$\|c_j\|^2$
|rrrrrrrrrrrrrr⟩	0:010
|rgrrrrrrrrrrrr⟩	0:006
|rrrrrrrrrrrrgr⟩	0:006
|rrrgrrrrrrrrrr⟩	0:006
|rrrrrrrrrrgrrr⟩	0:006

– = 2:5; n_S = 0:5	
$\|u_j\rangle$	$\|c_j\|^2$
|rrrrrrrrrrrrrr⟩	0:615
|rrgrrrrrrrrrrr⟩	0:021
|rrrrrrrrrrrgrr⟩	0:021
|rrrrrrrrrgrrrr⟩	0:021
|rrrrgrrrrrrrrr⟩	0:021

– = 4:5; n_S = 0:5	
$\|u_j\rangle$	$\|c_j\|^2$
|rrrrrrrrrrrrrr⟩	0:823
|rrrgrrrrrrrrrr⟩	0:012
|rrrrrrrrrgrrrr⟩	0:012
|rrrrrgrrrrrrrr⟩	0:012
|rrrrrrrrgrrrrr⟩	0:012

– = 0:5; n_S = 1:6	
$\|u_j\rangle$	$\|c_j\|^2$
|rgggggggggggr⟩	0:006
|rggrgggggggggr⟩	0:004
|rgggggggggrgg⟩	0:004
|ggggggggggggr⟩	0:004
|rgggggggggggg⟩	0:004

– = 2:5; n_S = 1:6	
$\|u_j\rangle$	$\|c_j\|^2$
|rgrgrgrggrgrgr⟩	0:168
|rgrgrggrgrgrgr⟩	0:168
|rgrgrgrgrggrgr⟩	0:118
|rgrggrgrgrgrgr⟩	0:118
|rggrgrgrgrgrgr⟩	0:049

– = 4:5; n_S = 1:6	
$\|u_j\rangle$	$\|c_j\|^2$
|rgrgrgrggrgrgr⟩	0:223
|rgrgrggrgrgrgr⟩	0:223
|rgrgrgrgrggrgr⟩	0:150
|rgrggrgrgrgrgr⟩	0:150
|rggrgrgrgrgrgr⟩	0:055

– = 0:5; n_S = 2:2	
$\|u_j\rangle$	$\|c_j\|^2$
|rgggggggggggr⟩	0:017
|rgggggggggggg⟩	0:015
|ggggggggggggr⟩	0:015
|ggggggggggggg⟩	0:014
|rgggggggggrgg⟩	0:011

– = 2:5; n_S = 2:2	
$\|u_j\rangle$	$\|c_j\|^2$
|rggrggrgggrggr⟩	0:149
|rggrgggrggrggr⟩	0:149
|rggrggrggrgggr⟩	0:071
|rgggrggrggrggr⟩	0:071
|rggrgggggggrgg⟩	0:030

– = 4:5; n_S = 2:2	
$\|u_j\rangle$	$\|c_j\|^2$
|rggrgrggrgrggr⟩	0:114
|rggrgrgrggrggr⟩	0:078
|rggrggrgrgrggr⟩	0:078
|rggrgrggrggrgr⟩	0:071
|rgrggrggrgrggr⟩	0:071

– = 0:5; n_S = 2:6	
$\|u_j\rangle$	$\|c_j\|^2$
|ggggggggggggg⟩	0:028
|rgggggggggggg⟩	0:027
|rgggggggggggg⟩	0:025
|ggggggggggggg⟩	0:025
|rgggrgggggggg⟩	0:014

– = 2:5; n_S = 2:6	
$\|u_j\rangle$	$\|c_j\|^2$
|rggrggrgggrggr⟩	0:218
|rggrgggrggrggr⟩	0:218
|rggrggrggrgggr⟩	0:115
|rgggrggrggrggr⟩	0:115
|rggrgggggggrgg⟩	0:038

– = 4:5; n_S = 2:6	
$\|u_j\rangle$	$\|c_j\|^2$
|rggrggrgggrggr⟩	0:304
|rggrgggrggrggr⟩	0:304
|rggrggrggrgggr⟩	0:130
|rgggrggrggrggr⟩	0:130
|rggrgggggggrgg⟩	0:023

– = 0:5; n_S = 3:7	
$|u_j\rangle$	$|c_j|^2$
|gggggggggggggig⟩	0:076
|grgggggggggggig⟩	0:050
|ggggggggggggigr⟩	0:050
|grgggggggggggir⟩	0:046
|ggggggggggggirg⟩	0:023

– = 2:5; n_S = 3:7	
$|u_j\rangle$	$|c_j|^2$
|grgggrggggrgggir⟩	0:240
|grggggrgggrgggir⟩	0:187
|grgggrgggrggggir⟩	0:187
|grgggggggrgggigr⟩	0:057
|grgggrgggggggigr⟩	0:057

– = 4:5; n_S = 3:7	
$|u_j\rangle$	$|c_j|^2$
|grgggrggggrgggir⟩	0:411
|grgggrgggrggggir⟩	0:232
|grggggrgggrggggir⟩	0:232
|grgggrgggggggigr⟩	0:028
|grgggggggrgggigr⟩	0:028

– = 0:5; n_S = 4:7	
$|u_j\rangle$	$|c_j|^2$
|gggggggggggggig⟩	0:112
|grgggggggggggig⟩	0:059
|ggggggggggggigr⟩	0:059
|grgggggggggggir⟩	0:041
|ggggggggggggirg⟩	0:032

– = 2:5; n_S = 4:7	
$|u_j\rangle$	$|c_j|^2$
|grgggggrgggggigr⟩	0:234
|grgggggrgggggigr⟩	0:234
|grgggggggggggigr⟩	0:088
|grgggggggrgggigr⟩	0:051
|grggggrgggggigr⟩	0:051

– = 4:5; n_S = 4:7	
$|u_j\rangle$	$|c_j|^2$
|grgggggrgggggigr⟩	0:329
|grgggggrgggggigr⟩	0:329
|grggggrgggggigr⟩	0:061
|grgggggggrgggigr⟩	0:061
|grgggggggggggigr⟩	0:052

A.5. N_{Atoms} = 15

– = 0:5; n_S = 0:5	
$|u_j\rangle$	$|c_j|^2$
|jrrrrrrrrrrrrrr i⟩	0:008
|jrgrrrrrrrrrrrr i⟩	0:005
|jrrrrrrrrrrrrgr i⟩	0:005
|jrrrrrrrrrrrgrrr i⟩	0:005
|jrrrgrrrrrrrrrr i⟩	0:005

– = 2:5; n_S = 0:5	
$|u_j\rangle$	$|c_j|^2$
|jrrrrrrrrrrrrrr i⟩	0:598
|jrrrrrrrrrrrrgrr i⟩	0:020
|jrrgrrrrrrrrrrr i⟩	0:020
|jrrrrrrrrrrgrrrr i⟩	0:020
|jrrrrgrrrrrrrrr i⟩	0:020

– = 4:5; n_S = 0:5	
$|u_j\rangle$	$|c_j|^2$
|jrrrrrrrrrrrrrr i⟩	0:809
|jrrrrrrrrrrrgrrr i⟩	0:012
|jrrrgrrrrrrrrrr i⟩	0:012
|jrrrrrgrrrrrrrr i⟩	0:012
|jrrrrrrrrrgrrrr i⟩	0:012

– = 0:5; n_S = 1:6	
$|u_j\rangle$	$|c_j|^2$
|grgggggggggggigr⟩	0:005
|ggggggggggggigr⟩	0:004
|grgggggggggggigg⟩	0:004
|grgggggggrgggigr⟩	0:003
|grggggrgggggggr⟩	0:003

– = 2:5; n_S = 1:6	
$|u_j\rangle$	$|c_j|^2$
|grgrgrgrgrgrgr i⟩	0:696
|grgrgrgggrgrgri⟩	0:032
|grgrgrgggrgrgri⟩	0:032
|grgrgggrgrgrgri⟩	0:032
|grgrgrgrgrgggri⟩	0:032

– = 4:5; n_S = 1:6	
$|u_j\rangle$	$|c_j|^2$
|grgrgrgrgrgrgr i⟩	0:846
|grgrgrgggrgrgri⟩	0:020
|grgrgrgggrgrgri⟩	0:020
|grgrgggrgrgrgri⟩	0:020
|grgrgrgrgrgggri⟩	0:020

$- = 0:5;\ n_S = 2:25$	
$\|u_j\rangle$	$\|c_j\|^2$
$\|rggggggggggggg\rangle$	0:014
$\|ggggggggggggg\rangle$	0:012
$\|ggggggggggggg\rangle$	0:012
$\|rggggggggggggg\rangle$	0:012
$\|rgggggggggrggg\rangle$	0:010

$- = 2:5;\ n_S = 2:25$	
$\|u_j\rangle$	$\|c_j\|^2$
$\|rggrggrgggrggr\rangle$	0:099
$\|rggrgggrggrggr\rangle$	0:099
$\|rggrggrgrggrgg\rangle$	0:087
$\|rggrggrggrgrgg\rangle$	0:069
$\|rggrgrggrggrgg\rangle$	0:069

$- = 4:5;\ n_S = 2:25$	
$\|u_j\rangle$	$\|c_j\|^2$
$\|rggrggrgrggrgg\rangle$	0:158
$\|rggrgrggrggrgg\rangle$	0:135
$\|rggrggrggrgrgg\rangle$	0:135
$\|rgrggrggrggrgg\rangle$	0:066
$\|rggrggrggrggrg\rangle$	0:066

$- = 0:5;\ n_S = 2:5$	
$\|u_j\rangle$	$\|c_j\|^2$
$\|ggggggggggggg\rangle$	0:019
$\|rggggggggggggg\rangle$	0:019
$\|ggggggggggggg\rangle$	0:017
$\|rggggggggggggg\rangle$	0:017
$\|rgggggggggrggg\rangle$	0:009

$- = 2:5;\ n_S = 2:5$	
$\|u_j\rangle$	$\|c_j\|^2$
$\|rggrgggrgggrgg\rangle$	0:107
$\|rggrgggrggrggg\rangle$	0:076
$\|rgggrggrgggrgg\rangle$	0:076
$\|rggrggrgggrggr\rangle$	0:064
$\|rggrggggrggrgg\rangle$	0:064

$- = 4:5;\ n_S = 2:5$	
$\|u_j\rangle$	$\|c_j\|^2$
$\|rggrggrgggrggr\rangle$	0:137
$\|rggrgggggrggrg\rangle$	0:137
$\|rggrggrgrggrgg\rangle$	0:093
$\|rggrggrggrgrgg\rangle$	0:070
$\|rggrgrggrggrgg\rangle$	0:070

$- = 0:5;\ n_S = 3$	
$\|u_j\rangle$	$\|c_j\|^2$
$\|ggggggggggggg\rangle$	0:034
$\|rggggggggggggg\rangle$	0:031
$\|ggggggggggggg\rangle$	0:029
$\|rggggggggggggg\rangle$	0:029
$\|rgggrgggggggggg\rangle$	0:013

$- = 2:5;\ n_S = 3$	
$\|u_j\rangle$	$\|c_j\|^2$
$\|rgggrggrggrggg\rangle$	0:116
$\|rggrgggrggrggg\rangle$	0:094
$\|rgggrggrgggrgg\rangle$	0:094
$\|rggrgggrgggrgg\rangle$	0:069
$\|rgggrgggggrggg\rangle$	0:059

$- = 4:5;\ n_S = 3$	
$\|u_j\rangle$	$\|c_j\|^2$
$\|rggrgggrggrggg\rangle$	0:169
$\|rgggrggrgggrgg\rangle$	0:169
$\|rggrgggrgggrgg\rangle$	0:161
$\|rgggrggrggrggg\rangle$	0:142
$\|rgggrgggrggrgg\rangle$	0:070

$- = 0:5;\ n_S = 4$	
$\|u_j\rangle$	$\|c_j\|^2$
$\|ggggggggggggg\rangle$	0:075
$\|ggggggggggggg\rangle$	0:048
$\|rggggggggggggg\rangle$	0:048
$\|rggggggggggggg\rangle$	0:038
$\|grggggggggggggg\rangle$	0:023

$- = 2:5;\ n_S = 4$	
$\|u_j\rangle$	$\|c_j\|^2$
$\|rggggrgggrgggg\rangle$	0:242
$\|rgggrgggggrggg\rangle$	0:147
$\|rggggrgggggrgg\rangle$	0:147
$\|rgggggggggrggg\rangle$	0:092
$\|rggggrgggggggg\rangle$	0:092

$- = 4:5;\ n_S = 4$	
$\|u_j\rangle$	$\|c_j\|^2$
$\|rggggrgggrgggg\rangle$	0:377
$\|rgggrgggggrggg\rangle$	0:236
$\|rggggrgggggrgg\rangle$	0:236
$\|rgggggrgggggrg\rangle$	0:031
$\|rgggggggggrggg\rangle$	0:031

B. Diagrams showing the Number of non-converging Ground State computations

For some combinations of h, n_S and N_{Sing} the implicitly restarted Lanczos method does not converge and thus aborts. This happens mostly for higher values of n_S and N_{Sing}. For $N_{Sing} < 30$ this didn't happen, since we have chosen $N_{Sing} = 20$ this problem doesn't affect us. The diagrams show for every value of $30 < N_{Sing} < 40$ how many of the 32 ground state computations corresponding to $h_{i;test}$ did not converge.

B.1. $N_{Atoms} = 11$

Figure 14: Plot showing for $30 < N_{Sing} < 40$ how many of the 32 approximated ground state computations did not converge. The system is of size $N_{Atoms} = 11$

B.2. $N_{Atoms} = 12$

Figure 15: Plot showing $3 < N_{Sing} < 40$ how many of the 32 approximated ground state computations did not converge. The system is of size $N_{Atoms} = 12$

B.3. $N_{Atoms} = 13$

Figure 16: Plot showing $3 < N_{Sing} < 40$ how many of the 32 approximated ground state computations did not converge. The system is of size $N_{Atoms} = 13$

B.4. $N_{Atoms} = 14$

Figure 17: Plot showing $3 < N_{Sing} < 40$ how many of the 32 approximated ground state computations did not converge. The system is of size $N_{Atoms} = 14$

B.5. $N_{Atoms} = 15$

Figure 18: Plot showing $3 < N_{Sing} < 40$ how many of the 32 approximated ground state computations did not converge. The system is of size $N_{Atoms} = 15$

C. Plots showing the Speedup of the SVD Approximation with Standard Deviation

The following plots show the relationship between computation time for exact ground states and approximated ground states. The errorbars go into the negative, because the standard deviation for $\overline{t_{gs;exact}}$ is bigger than $\overline{t_{gs;exact}}$ itself. This is because the values of $t_{gs;exact}$ span several orders of magnitude depending on the two parameters – and n_S.

C.1. $N_{Atoms} = 11$

Figure 19: Plot showing the relationship between $\overline{t_{gs;exact}}$ and $\overline{t_{gs;approx}}$ with uncertainty for 11 atoms. $\overline{t_{gs;exact}}$ is the mean time it takes to compute an exact ground state. $\overline{t_{gs;approx}}$ is the mean time it takes to compute an approximated ground state. N_{Sing} is the number of singular values considered for the SVD approximation.

C.2. $N_{Atoms} = 12$

Figure 20: Plot showing the relationship between $\overline{t_{gs;exact}}$ and $\overline{t_{gs;approx}}$ with uncertainty for 12 atoms. $\overline{t_{gs;exact}}$ is the mean time it takes to compute an exact ground state. $\overline{t_{gs;approx}}$ is the mean time it takes to compute an approximated ground state. N_{Sing} is the number of singular values considered for the SVD approximation.

C.3. $N_{Atoms} = 13$

Figure 21: Plot showing the relationship between $\overline{t_{gs;exact}}$ and $\overline{t_{gs;approx}}$ with uncertainty for 13 atoms. $\overline{t_{gs;exact}}$ is the mean time it takes to compute an exact ground state. $\overline{t_{gs;approx}}$ is the mean time it takes to compute an approximated ground state. N_{Sing} is the number of singular values considered for the SVD approximation.

C.4. $N_{Atoms} = 14$

Figure 22: Plot showing the relationship between $\overline{t_{gs;exact}}$ and $\overline{t_{gs;approx}}$ with uncertainty for 14 atoms. $\overline{t_{gs;exact}}$ is the mean time it takes to compute an exact ground state. $\overline{t_{gs;approx}}$ is the mean time it takes to compute an approximated ground state. N_{Sing} is the number of singular values considered for the SVD approximation.

C.5. $N_{Atoms} = 15$

Figure 23: Plot showing the relationship between $\overline{t_{gs;exact}}$ and $\overline{t_{gs;approx}}$ with uncertainty for 15 atoms. $\overline{t_{gs;exact}}$ is the mean time it takes to compute an exact ground state. $\overline{t_{gs;approx}}$ is the mean time it takes to compute an approximated ground state. N_{Sing} is the number of singular values considered for the SVD approximation.

D. Plots showing the mean Accuracy of SVD Approximations depending on N_{Sing}

D.1. $N_{Atoms} = 11$

Figure 24: Plot showing the mean accuracy $_{mean}$ of the SVD approximation with standard deviation across all test points $\pm 2 f \sigma_{i;test} g$, depending on N_{Sing} for $N_{Atoms} = 11$

D.2. $N_{Atoms} = 12$

Figure 25: Plot showing the mean accuracy $_{mean}$ of the SVD approximation with standard deviation across all test points $\mu \in \{\mu_{i,test}\}$, depending on N_{Sing} for $N_{Atoms} = 12$

D.3. $N_{Atoms} = 13$

Figure 26: Plot showing the mean accuracy $_{mean}$ of the SVD approximation with standard deviation across all test points $\in \{n \mid n \in \mathbb{N}_{;test}\}$, depending on N_{Sing} for $N_{Atoms} = 13$

D.4. $N_{Atoms} = 14$

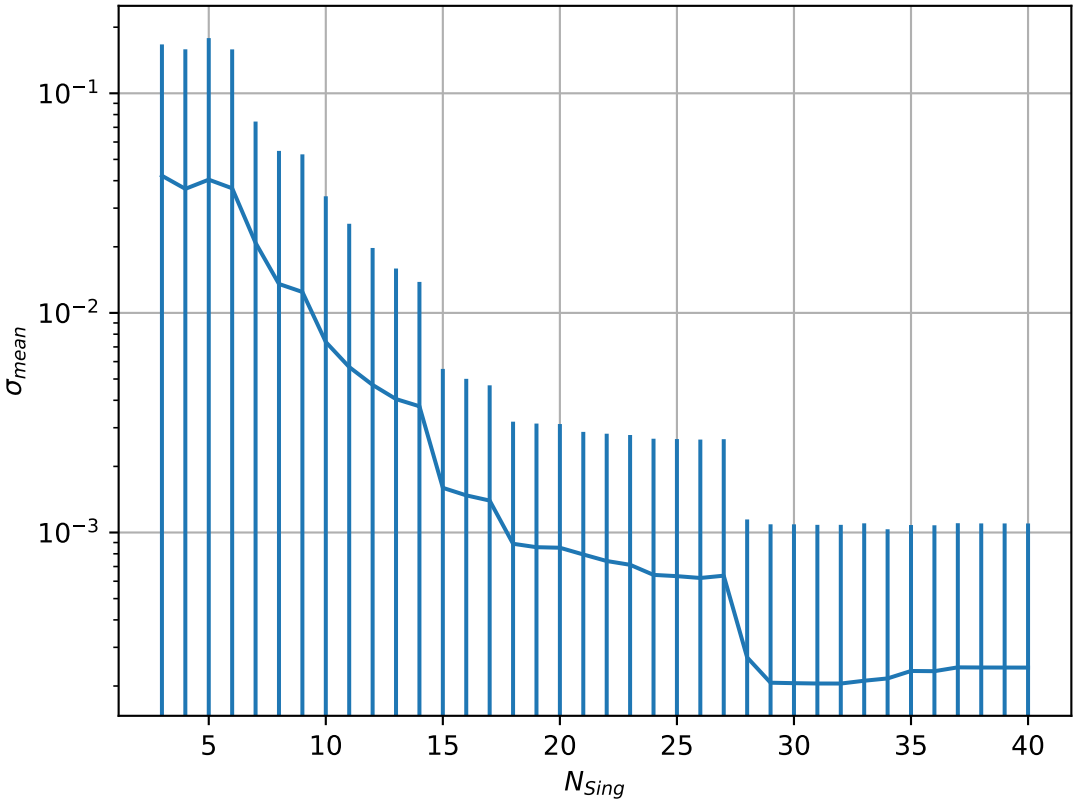

Figure 27: Plot showing the mean accuracy $_{mean}$ of the SVD approximation with standard deviation across all test points p_i 2 $fp_{i;test}g$, depending on N_{Sing} for $N_{Atoms} = 14$

D.5. $N_{Atoms} = 15$

Figure 28: Plot showing the mean accuracy $_{mean}$ of the SVD approximation with standard deviation across all test points $p_i \ 2 \ fp_{i;test}g$, depending on N_{Sing} for $N_{Atoms} = 15$

References

[1] David D Awschalom, Lee C Bassett, Andrew S Dzurak, Evelyn L Hu, and Jason R Petta. Quantum spintronics: engineering and manipulating atom-like spins in semiconductors. Science, 339(6124):1174–1179, 2013.

[2] Hannes Bernien, Sylvain Schwartz, Alexander Keesling, Harry Levine, Ahmed Omran, Hannes Pichler, Soonwon Choi, Alexander S Zibrov, Manuel Endres, Markus Greiner, et al. Probing many-body dynamics on a 51-atom quantum simulator. Nature, 551(7682):579–584, 2017.

[3] Antoine Browaeys and Thierry Lahaye. Many-body physics with individually controlled Rydberg atoms. Nature Physics, pages 1–11, 2020.

[4] Daniela Calvetti, L Reichel, and And Sorensen. An implicitly restarted Lanczos method for large symmetric eigenvalue problems. Electronic Trans. Numer. Anal., 2:1–21, 04 1994.

[5] The NumPy Community. Numpy (version 1.18.5), 2020. URL `https://github.com/numpy/numpy`.

[6] The SciPy Community. Numpy v1.19 manual, 2020. URL `https://numpy.org/doc/stable/`. (accessed: 14.11.2020).

[7] The SciPy Community. numpy.linalg.svd, 2020. URL `https://numpy.org/doc/stable/reference/generated/numpy.linalg.svd.html`. (accessed: 22.11.2020).

[8] The SciPy Community. Scipy (version 1.4.1), 2020. URL `https://github.com/scipy/scipy`.

[9] The SciPy Community. Scipy reference guide, 2020. URL `https://docs.scipy.org/doc/scipy/reference/`. (accessed: 02.11.2020).

[10] The SciPy Community. scipy.sparse.linalg.eigsh, 2020. URL `https://docs.scipy.org/doc/scipy/reference/generated/scipy.sparse.linalg.eigsh.html`. (accessed: 02.11.2020).

[11] Ph. W. Courteille. Interaction of light with cold atoms, 2019. URL `http://www.ifsc.usp.br/~strontium/Publication/Scripts/LightAtomsLecture.pdf`. (accessed: 26.10.2020).

[12] D.C. Sorensen, R.B. Lehoucq, C. Yang, and K. Maschhoff. Arpack software, 2008. URL `https://www.caam.rice.edu/software/ARPACK/`.

[13] Michel H Devoret and Robert J Schoelkopf. Superconducting circuits for quantum information: an outlook. Science, 339(6124):1169–1174, 2013.

[14] David P DiVincenzo. The physical implementation of quantum computation. Fortschritte der Physik: Progress of Physics, 48(9-11):771–783, 2000.

[15] Carl Eckart and Gale Young. The approximation of one matrix by another of lower rank. Psychometrika, 1(3):211–218, 1936.

[16] Francisco Fernández. The Kronecker product and some of its physical applications. European Journal of Physics, 37:065403, 11 2016. doi: 10.1088/0143-0807/37/6/065403.

[17] Gene H Golub and Charles F Van Loan. Matrix computations, 4th. Johns Hopkins, 2013.

[18] Paul R Halmos. Finite-dimensional vector spaces. Courier Dover Publications, 2017.

[19] Jim Hefferon. Linear algebra fourth edition. 2020.

[20] L Isenhower, E Urban, XL Zhang, AT Gill, T Henage, Todd A Johnson, TG Walker, and M Saffman. Demonstration of a neutral atom controlled-NOT quantum gate. Physical review letters, 104(1):010503, 2010.

[21] Richard M Johnson. On a theorem stated by Eckart and Young. Psychometrika, 28(3):259–263, 1963.

[22] Henning Labuhn, Daniel Barredo, Sylvain Ravets, Sylvain De Léséleuc, Tommaso Macrì, Thierry Lahaye, and Antoine Browaeys. Tunable two-dimensional arrays of single Rydberg atoms for realizing quantum Ising models. Nature, 534(7609): 667–670, 2016.

[23] Cornelius Lanczos. An iteration method for the solution of the eigenvalue problem of linear differential and integral operators. United States Governm. Press Office Los Angeles, CA, 1950.

[24] Richard B Lehoucq, Danny C Sorensen, and Chao Yang. ARPACK users' guide: solution of large-scale eigenvalue problems with implicitly restarted Arnoldi methods. SIAM, 1998.

[25] Christopher Monroe and Jungsang Kim. Scaling the ion trap quantum processor. Science, 339(6124):1164–1169, 2013.

[26] Wolfgang Nolting. Theoretical Physics 6. Springer, 2017.

[27] Wolfgang Nolting. Theoretical Physics 7: Quantum Mechanics-Methods and Applications. Springer, 2017.

[28] Jonathan D Pritchard, D Maxwell, Alexandre Gauguet, Kevin J Weatherill, MPA Jones, and Charles S Adams. Cooperative atom-light interaction in a blockaded Rydberg ensemble. Physical review letters, 105(19):193603, 2010.

[29] Mark Saffman. Quantum computing with atomic qubits and Rydberg interactions: progress and challenges. Journal of Physics B: Atomic, Molecular and Optical Physics, 49(20):202001, 2016.

[30] Peter Schauß, Marc Cheneau, Manuel Endres, Takeshi Fukuhara, Sebastian Hild, Ahmed Omran, Thomas Pohl, Christian Gross, Stefan Kuhr, and Immanuel Bloch. Observation of spatially ordered structures in a two-dimensional Rydberg gas. Nature, 491(7422):87–91, 2012.

[31] Peter Schauß, Johannes Zeiher, Takeshi Fukuhara, Sebastian Hild, Marc Cheneau, Tommaso Macrì, Thomas Pohl, Immanuel Bloch, and Christian Groß. Crystallization in Ising quantum magnets. Science, 347(6229):1455–1458, 2015.

[32] John Von Neumann. Mathematical foundations of quantum mechanics: New edition. Princeton university press, 2018.

[33] Tatjana Wilk, A Gaëtan, C Evellin, J Wolters, Y Miroshnychenko, P Grangier, and A Browaeys. Entanglement of two individual neutral atoms using Rydberg blockade. Physical Review Letters, 104(1):010502, 2010.

[34] Johannes Zeiher, Jae-yoon Choi, Antonio Rubio-Abadal, Thomas Pohl, Rick van Bijnen, Immanuel Bloch, and Christian Gross. Coherent many-body spin dynamics in a long-range interacting Ising chain. Physical Review X, 7(4):041063, 2017.